NASA Technical Paper 2613

December 1986

A Second-Order Accurate Kinetic-Theory-Based Method for Inviscid Compressible Flows

Suresh M. Deshpande

NASA

NASA
Technical
Paper
2613

1986

A Second-Order Accurate Kinetic-Theory-Based Method for Inviscid Compressible Flows

Suresh M. Deshpande

Langley Research Center
Hampton, Virginia

NASA
National Aeronautics
and Space Administration

**Scientific and Technical
Information Branch**

Summary

A new upwind method for the numerical solution of the Euler equations is presented. This method, called the kinetic numerical method (KNM), is based on the well-known fact that the Euler equations are the moments of the Boltzmann equation of the kinetic theory of gases when the distribution function is Maxwellian. The KNM consists of two phases, the convection phase and the collision phase. The velocity distribution function at the end of the convection phase is the solution of the collisionless Boltzmann equation, which is linear and hyperbolic. The collision phase instantaneously relaxes the distribution to the local Maxwellian distribution. The fluid dynamic variables of density, velocity, and internal energy are obtained as moments of the velocity distribution function at the end of the convection phase. The KNM is an explicit method and is unconditionally stable. It is an upwind method because of the way the solution is obtained in the convection phase and satisfies the entropy condition due to the convexity of the Boltzmann H-function, which decreases as the velocity distribution function suddenly relaxes to the local Maxwellian distribution during the collision phase. Because of its explicit nature, the KNM is highly vectorizable and can be easily made into a total variation diminishing (TVD) method for the distribution function through a suitable choice of the interpolation strategy.

A fascinating aspect of the present work is the use of the antidiffusive Chapman-Enskog theory in the development of the second-order accurate KNM. Normally the Chapman-Enskog theory is associated with the Navier-Stokes equations, and use of the Chapman-Enskog theory for constructing the second-order KNM is very unusual. It is shown that to cancel the large amount of viscosity in the first-order KNM, antidiffusive terms are required, and these can be introduced through the Chapman-Enskog distribution if the shear stress tensor $\boldsymbol{\tau}$ and heat flux vector $\mathbf{q}$ are made antidiffusive. Through the addition of diffusive terms corresponding to viscosity and heat conduction to the expressions for $\boldsymbol{\tau}$ and $\mathbf{q}$ used in the Chapman-Enskog distribution, the KNM can be easily extended to the solution of the Navier-Stokes equations.

The KNM is applied to a one-dimensional shock-propagation problem, and the results demonstrate the capability of the method for giving "wiggle-free" accurate solutions. Also, the Euler space-marching KNM is applied to obtain the steady solution to a shock-reflection problem. In this application, the boundary condition is treated differently from other finite-difference methods in that the flow tangency condition at the flat plate is imposed by reversing the normal velocity of the reflected molecules. The boundary condition is at the level of the velocity distribution function, which is natural in the KNM. The pressure profiles are compared with a second-order and a third-order accurate TVD method, and the ability of the KNM to yield an accurate wiggle-free solution is demonstrated.

Introduction

Recently, several numerical methods based on kinetic theory have been proposed for the computation of inviscid compressible flows (refs. 1 to 4). These methods use the Boltzmann or the Boltzmann-like equation of the kinetic theory of gases. These kinetic numerical methods (KNM's), as Aristov and Tcheremissine (ref. 4) call them, are based on the connection between the Boltzmann equation and the Euler equations governing the dynamics of inviscid compressible flows. The basic unknown in the Boltzmann equation is the velocity distribution function $f(t, \mathbf{x}, \mathbf{v}, I)$, where t is time, $\mathbf{x}$ is the position vector, $\mathbf{v}$ is the molecular velocity vector, and I is the independent internal-energy variable corresponding to nontranslational degrees of freedom. The spatio-temporal evolution of f is governed by the Boltzmann equation

$$\frac{\partial f}{\partial t} + \mathbf{v} \cdot \frac{\partial f}{\partial \mathbf{x}} = J(f, f) \tag{1}$$

Equation (1) consists of the streaming, or convective, term $\left(\frac{\partial}{\partial t} + \mathbf{v} \cdot \frac{\partial}{\partial \mathbf{x}}\right) f$ and the collision term $J(f, f)$. The convective term gives the rate of change of f per unit volume in $(\mathbf{x}, \mathbf{v}, I)$ space because of movement of molecules, and the collision term gives the rate of change of f because of intermolecular collisions.

The field variables ρ, $\mathbf{u}$, and e (which are, respectively, the mass density, the fluid velocity vector, and the specific total internal energy) are related to f through moment equations (see appendix A). It is shown in appendix A that the moments of the Boltzmann equation (1) are the Euler equations if the velocity distribution function f is the Maxwellian distribution F as follows:

$$f = F = \frac{\rho}{(2\pi RT)^{3/2}} \exp\left[-\frac{(\mathbf{v} - \mathbf{u})^2}{2RT}\right] \frac{\exp\left(-I/I_o\right)}{I_o} \tag{2}$$

where R is the gas constant, T is the temperature, I is the internal-energy variable corresponding to nontranslational degrees of freedom,

$$I_o = \frac{(2 + D_f) - \gamma D_f}{2(\gamma - 1)} RT$$

D_f is the degrees of freedom of a molecule, and γ is the ratio of specific heats. It is interesting to note here that if f is assumed to be the Chapman-Enskog distribution (ref. 5), then the moment equations reduce to the Navier-Stokes equations. This connection between the Boltzmann equation and the equations of fluid dynamics is the basis of all KNM's.

Several variants of KNM's can be obtained by adopting particle-in-cell (PIC), fluid-in-cell (FLIC), or finite-difference methods. Pullin (ref. 1) follows the statistical PIC method, in which the computational domain is divided into several Eulerian cells. The fluid is represented in the PIC method by a large number of discrete Lagrangian mass points, called particles, which move through the Eulerian mesh convecting mass, momentum, and energy. The velocities of these particles are drawn from the local Maxwellian velocity distribution function at the end of each time step Δt, thus ensuring the time evolution of $\rho, \mathbf{u}$, and T by the Euler equations. Obviously, like the PIC method of Evans and Harlow (ref. 6), this method requires very long computation times. In addition, the Eulerian field variables are subject to statistical scatter. As Rich and Blackman (ref. 7) modified the PIC method and obtained the FLIC method for considerably improving the efficiency, Pullin (ref. 1) also investigated FLIC-like methods. In this variant, cells interact with their immediate neighbors through exchange of mass, momentum, and energy calculated with the Maxwellian distribution. Because the functional form for f is explicitly known, it is possible to calculate these fluxes by using analytical formulas involving error functions. It is expected that this FLIC variant will require less computational time and the unknowns will be free of statistical fluctuations. However, as observed by Deshpande and Raul (ref. 3), this method is only first-order accurate in both space and time and has the same stability restriction on Δt as other explicit finite-difference methods. The primary reason for the restriction on Δt is that this method permits fluid movement to immediate neighbors only. The true physical situation, however, is that the particles can move from a cell to any other cell. This is particularly important in high-speed flows. It would be highly worthwhile to develop a new FLIC variant of the KNM to allow multicell interaction, that is, interaction between a cell and its first neighbors, its second neighbors, and so forth. Such a method can be expected to possess a much less restrictive stability limit on the time step.

There is one more reason why multicell interaction is desirable. It is well-known that almost all explicit numerical methods are very efficient in eliminating small-scale errors (i.e., errors with wavelengths of the order of mesh size) but are very slow in eliminating large-scale errors. This is the primary reason behind the slow convergence to the steady state. A FLIC method involving multicell interaction is expected to converge rapidly to the steady state. The kinetic theory based fluid-in-cell (KTFLIC) method of Deshpande and Raul (ref. 3) allows multicell interaction. The transport of mass, momentum, and energy from a cell to any other cell can be obtained in closed form by integrating an appropriate flux relation involving the local Maxwellian distribution. The KNM of Reitz (ref. 2) also involves interaction between a mesh point and any other mesh point. This method is very similar, in principle, to the KTFLIC method and it involves integration over velocity only. The KTFLIC, on the other hand, requires integration over both velocity and space. The KNM of Reitz is more efficient than the methods of references 1 and 3.

The KNM's of Reitz (ref. 2) and of Deshpande and Raul (ref. 3) are explicit and unconditionally stable. Preliminary computations on a one-dimensional shock-tube problem (refs. 2 and 3) show that the numerical solution does not exhibit pre- and post-shock oscillations. There is one major disadvantage, however, in the methods of references 1, 2, and 3, namely, the magnitude of the numerical diffusion is proportional to the time step. This restricts the use of a large time step in spite of the unconditional stability. Further, with the true physical diffusion being proportional to the mean collision time, any extension of the method to the viscous case will imply that unusually small values of the time step are required.

The present paper studies the KNM of references 2 and 3 from a theoretical point of view and demonstrates that the method is upwinding, satisfies the entropy condition, and is total variation nonincreasing (TVNI). The entropy condition is satisfied because of the existence of a convex H-function defined by Boltzmann in establishing the famous H-theorem (ref. 8). Further, the question of numerical diffusion is studied in considerable detail. It is shown that if the basic premise of the distribution function is replaced by the Chapman-Enskog distribution (with a suitably defined stress tensor $\boldsymbol{\tau}$ and heat flux vector $\mathbf{q}$), then the KNM can be made second-order accurate in space and time. The numerical diffusion in this new variant is of the order of Δt^2. The use of the Chapman-Enskog theory in developing the second-order accurate KNM for the solution of inviscid flows is very surprising. The Chapman-Enskog theory is always associated with the Navier-Stokes equations. In fact, Pullin (ref. 1) has referred to the use of the Chapman-Enskog theory for the treatment of viscous and heat-conduction effects. Reitz (ref. 2)

has used the Chapman-Enskog distribution to correct for diffusional effects. The present paper, on the other hand, uses the Chapman-Enskog theory to develop a more accurate KNM for the purpose of solving inviscid flow problems. The Chapman-Enskog terms are antidiffusive in nature and are a perturbation over the Maxwellian distribution so that the large viscosity of the first-order KNM is cancelled by them. Finally, the KNM is extended to the case of steady, inviscid supersonic flow. Because of the hyperbolicity of the equations in this case, the KNM becomes an Euler space-marching method.

Symbols and Abbreviations

a	speed of sound
B	$= \frac{3-\gamma}{4(\gamma-1)}$
C	normalized peculiar velocity
c	peculiar velocity
$\tilde{c}$	$= \frac{v_2}{v_1}$
D_f	degrees of freedom of a molecule
e	specific internal energy
F	Maxwellian distribution
$\tilde{F}$	contracted local Maxwellian distribution
f	velocity distribution function
$\bar{f}, \bar{\bar{f}}$	distributions related to f
$\tilde{f}$	contracted velocity distribution function
H	Boltzmann H-function
H_v	flux of H
I	internal-energy variable due to nontranslational degrees of freedom
I_o	internal energy due to nontranslational degrees of freedom
J	Boltzmann collision term; number of mesh points
KNM	kinetic numerical method
M_1	Mach number
n	time level
P_q	Chapman-Enskog polynomial corresponding to $\mathbf{q}$
P_τ	Chapman-Enskog polynomial corresponding to $\boldsymbol{\tau}$
p	pressure
$\mathbf{q}$	heat flux vector
R	gas constant per unit mass
r_D	ratio of backward to forward difference of f
T	temperature
TV	total variation
TVD	total variation diminishing
TVNI	total variation nonincreasing
t	time coordinate
t_A	time up to which solution is advanced
U	conserved variable
$\mathbf{u}$	fluid velocity vector
u_1, u_2	components of fluid velocity in directions 1 and 2
$\mathbf{v}$	molecular velocity vector
v_1, v_2, v_3	components of molecular velocity in directions 1, 2, and 3
X_1, X_2	axes in directions 1 and 2
$\mathbf{x}$	position vector
x_1, x_2	coordinates in directions 1 and 2
$x_{1,L}, x_{1,U}$	lower and upper bounds on x_1
$x_{2,L}, x_{2,U}$	lower and upper bounds on x_2
α	time constant characteristic of collisions
β	inverse of $2RT$
γ	ratio of specific heats
Δt	increment in t
Δx	increment in $\mathbf{x}$
δ	angle of deflection
ρ	mass density
$\boldsymbol{\tau}$	viscous stress tensor
Φ	multiplier of Maxwellian distribution in Chapman-Enskog theory

ϕ	general function
Ψ	moment function (see eq. (80))
ψ	collisional invariants
Subscripts:	
CE	Chapman-Enskog
HP	high-pressure side of shock tube
i, j	mesh points
LP	low-pressure side of shock tube
Superscripts:	
$\overline{n+1}$	intermediate level between n and $n+1$

One prime indicates the first derivative and two primes indicate the second derivative of a quantity.

Kinetic Numerical Method

For studying the basic aspects of the kinetic numerical method (KNM), only one-dimensional flow is considered now. The Boltzmann equation (1) reduces to

$$\frac{\partial f}{\partial t} + v\frac{\partial f}{\partial x} = J(f,f) \tag{3}$$

The velocity distribution $f = f(t,x,v,I)$ is now a function of four variables. The moments ρ, u, e, τ, and q are defined by

$$\left.\begin{aligned}
\rho = \rho(t,x) &= \int_{-\infty}^{\infty} dv \int_0^{\infty} dI\ (f) \\
\rho \mathbf{u} &= \int_{-\infty}^{\infty} dv \int_0^{\infty} dI\ (vf) \\
\rho e &= \int_{-\infty}^{\infty} dv \int_0^{\infty} dI \left(I + \frac{v^2}{2}\right) f \\
p - \tau &= \int_{-\infty}^{\infty} dv \int_0^{\infty} dI\,(v-u)^2 f \\
q &= -\int_{-\infty}^{\infty} dv \int_0^{\infty} dI \left[I + \frac{(v-u)^2}{2}\right](v-u)f
\end{aligned}\right\} \tag{4}$$

In the Euler limit,

$$J(f,f) = 0$$

and the distribution f is then the Maxwellian distribution:

$$f = F = \frac{\rho}{I_o(2\pi RT)^{1/2}} \exp\left[-\frac{(v-u)^2}{2RT} - \frac{I}{I_o}\right] \tag{5}$$

where $I_o = \frac{3-\gamma}{2(\gamma-1)}RT$ for $D_f = 1$. A solution scheme for equation (3) can be constructed by splitting the equation as follows:

$$\frac{\partial f}{\partial t} = -v\frac{\partial f}{\partial x} \tag{6}$$

$$\frac{\partial f}{\partial t} = J(f,f) \tag{7}$$

With the distribution function at time level n denoted by $f^n(x,v,I)$, the solution of equation (6) is given by

$$f^{\overline{n+1}}(x,v,I) = f^n(x - v\,\Delta t, v, I) \tag{8}$$

Note that equation (8) is an exact solution of equation (6), which is a collisionless Boltzmann equation. In the Euler limit, $J(f,f) = 0$. The vanishing of J is due to a very large number of intermolecular collisions. Because $J = 0$ if and only if f is a Maxwellian distribution, it follows that the solution of equation (7) in the Euler limit is

$$F^{n+1}(x,v) = F\left(f^{\overline{n+1}}\right) \tag{9}$$

where $F\left(f^{\overline{n+1}}\right)$ is the local Maxwellian distribution with ρ, u, and e the same as those of $f^{\overline{n+1}}$, that is,

$$\iint \begin{bmatrix} 1 \\ v \\ I + \frac{v^2}{2} \end{bmatrix} \left(F^{n+1} - f^{\overline{n+1}}\right) dv\, dI = 0 \tag{10}$$

The method thus consists of two phases, the convection phase and the collision phase. In the convection phase, the fluid particles located at $x - v\,\Delta t$ are moved to x, whereas in the collision phase the resultant distribution function after convection immediately relaxes to the local Maxwellian distribution. In view of the conservation of mass, momentum, and energy during the collision phase, the first three moments of F^{n+1} are the same as those of $f^{\overline{n+1}}$. Therefore, the KNM can be written as

$$\left.\begin{aligned}
\rho_j^{n+1} &= \int_{-\infty}^{\infty} dv \int_0^{\infty} dI\, F\left(t_n, x_j - v\,\Delta t, I\right) \\
(\rho u)_j^{n+1} &= \int_{-\infty}^{\infty} dv \int_0^{\infty} dI\, vF\left(t_n, x_j - v\,\Delta t, I\right) \\
(\rho e)_j^{n+1} &= \int_{-\infty}^{\infty} dv \int_0^{\infty} dI \left(I + \frac{v^2}{2}\right) F\left(t_n, x_j - v\,\Delta t, I\right)
\end{aligned}\right\} \tag{11}$$

where the standard notation $\rho_j^n = \rho\left(t_n, x_j\right)$ has been used. The integration with respect to the variable I yields

$$\left.\begin{aligned} \rho_j^{n+1} &= \int_{-\infty}^{\infty} dv\, \tilde{F}\left(t_n, x_j - v\,\Delta t\right) \\ (\rho u)_j^{n+1} &= \int_{-\infty}^{\infty} dv\, v\tilde{F}\left(t_n, x_j - v\,\Delta t\right) \\ (\rho e)_j^{n+1} &= \int_{-\infty}^{\infty} dv \left[I_o\left(t_n, x_j - v\,\Delta t\right) + \frac{v^2}{2}\right] \\ &\quad \times \tilde{F}\left(t_n, x_j - v\,\Delta t\right) \end{aligned}\right\} \qquad (12)$$

where $\tilde{F}$ is the contracted local Maxwellian distribution defined by

$$\tilde{F} = \rho\left(\frac{\beta}{\pi}\right)^{1/2} \exp\left[-\beta(v-u)^2\right] \qquad (13)$$

where $\beta = \frac{1}{2RT}$. Equations (12) are basic relations of the KNM. The field variables ρ, u, and T are stored at mesh points only, and therefore $\tilde{F}\left(x_j - v\,\Delta t\right)$ has to be determined by some kind of interpolation (unless $x_j - v\,\Delta t$ is chosen to coincide with another mesh point). One choice for interpolation is

$$\tilde{F}\left(x_j - v\,\Delta t\right) = \tilde{F}_i(1-\xi) + \tilde{F}_{i+1}\xi \qquad (14)$$

where $x_j - v\,\Delta t = x_i + \xi\,\Delta t$ for $0 \le \xi \le 1$. The relationship between x_i, x_j, and ξ is shown in the sketch below.

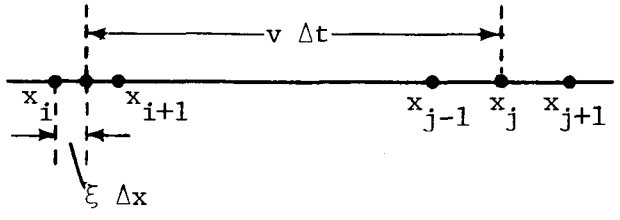

It is possible that the point $x_j - v\,\Delta t$ is outside the computational domain, that is, the fluid particle has crossed the domain boundaries during convection. Obviously, a boundary strategy is then required to find $\tilde{F}(x_j - v\,\Delta t)$ so that physically meaningful desired boundary conditions are satisfied. A discussion of how to specify boundary conditions is given later.

The interpolation formula (eq. (14)) is only first-order accurate in space and equation (8) is only first-order accurate in time. Hence, the KNM (eqs. (12)) for the solution of the Euler equations is first-order accurate in space and time. It is shown subsequently that to achieve second-order accuracy it is not enough to use a second-order accurate interpolation formula.

A few important properties of equations (12) are worth noting. The implementation of equations (12) involves only quadrature, and no numerical differentiation is required. Because of the long-range interaction among mesh points the method, despite being explicit, is expected to be unconditionally stable. Indeed, Reitz (ref. 2) and Harten, Lax, and van Leer (ref. 9) have shown that methods of the type of equations (12) are unconditionally stable. Also, the method possesses a high degree of vectorization because it is explicit and dominated by arithmetic operations rather than logic. The vector code is, in fact, about 8 times faster than the scalar code for a one-dimensional shock-tube problem with 500 mesh points.

Properties of the KNM

At this point, it would be interesting to investigate whether the KNM has other important properties like upwinding, entropy condition satisfaction, and TVNI. Of late, development of schemes possessing these properties is considered highly desirable because of many advantages. For example, an upwind method is robust and has a lot of physical appeal (ref. 9). A method satisfying the entropy condition prevents formation of expansion shocks. Further, if a method is TVNI then the solution is free from pre- and post-shock oscillations. In the case of the KNM, the upwinding nature is a direct consequence of equation (8), which states that the solution at any mesh point is influenced by the data upwind of that point. As mentioned in the *Introduction*, an H-function can be defined which satisfies the entropy condition. The demonstration of this capability proceeds as follows.

The Boltzmann H-theorem has been described in the kinetic theory of gases as the bridge connecting the equilibrium thermodynamics with the nonequilibrium statistical mechanics. Briefly stated, it says that the H-function defined by

$$H = \iiint f \ln f \, dv_1\, dv_2\, dv_3 \qquad (15)$$

monotonically decreases with time as a homogeneous gas in statistical nonequilibrium evolves to equilibrium. In the case of spatial inhomogeneity, the theorem states that

$$\frac{\partial H}{\partial t} + \sum_i \frac{\partial H_i}{\partial x_i} \le 0$$

where H_i is the H-flux defined by

$$H_i = \iiint v_i f \ln f \, dv_1 \, dv_2 \, dv_3$$

For the one-dimensional case we therefore define

$$\left.\begin{aligned} H &= \iint \left[F \ln F + \frac{5-3\gamma}{2(\gamma-1)} F \ln \beta\right] dv \, dI \\ H_v &= \iint v \left[F \ln F + \frac{5-3\gamma}{2(\gamma-1)} F \ln \beta\right] dv \, dI \end{aligned}\right\} \tag{16}$$

Note that an additional term involving $F \ln \beta$ is required to account for nontranslational degrees of freedom. (See ref. 8.) From equations (16) we obtain

$$\begin{aligned} \frac{\partial H}{\partial t} + \frac{\partial H_v}{\partial x} = &\iint (1 + \ln F) \left(\frac{\partial F}{\partial t} + v \frac{\partial F}{\partial x}\right) dv \, dI \\ &+ \frac{5-3\gamma}{2(\gamma-1)} \iint \left(\frac{\partial}{\partial t} + v \frac{\partial}{\partial x}\right) \\ &\times (F \ln \beta) dv \, dI \end{aligned} \tag{17}$$

Now,

$$\int \beta I \left(\frac{\partial F}{\partial t} + v \frac{\partial F}{\partial x}\right) dv \, dI = \int \beta \left[\frac{\partial}{\partial t} \left(I_o \tilde{F}\right) + v \frac{\partial}{\partial x} \left(I_o \tilde{F}\right)\right] dv \tag{18}$$

where $\tilde{F}$ is the contracted local Maxwellian distribution defined in equation (13). Substituting for I_o in terms of β, we get

$$\begin{aligned} \iint \beta I \left(\frac{\partial F}{\partial t} + v \frac{\partial F}{\partial x}\right) dv \, dI = &\int \frac{3-\gamma}{4(\gamma-1)} \beta \left[\frac{\partial}{\partial t} \left(\frac{\tilde{F}}{\beta}\right)\right. \\ &\left. + v \frac{\partial}{\partial x} \left(\frac{\tilde{F}}{\beta}\right)\right] dv \\ = &\frac{3-\gamma}{4(\gamma-1)} \int \left[\frac{\partial \tilde{F}}{\partial t} + v \frac{\partial \tilde{F}}{\partial x}\right. \\ &\left. - \tilde{F} \left(\frac{\partial}{\partial t} \ln \beta + v \frac{\partial}{\partial x} \ln \beta\right)\right] dv \\ = &\frac{3-\gamma}{4(\gamma-1)} \int (1 + \ln \beta) \\ &\times \left(\frac{\partial \tilde{F}}{\partial t} + v \frac{\partial \tilde{F}}{\partial x}\right) dv \\ &- \frac{3-\gamma}{4(\gamma-1)} \int \left[\frac{\partial}{\partial t} (\tilde{F} \ln \beta)\right. \\ &\left. + v \frac{\partial}{\partial x} (\tilde{F} \ln \beta)\right] \end{aligned} \tag{19}$$

Noting that the equation of continuity is

$$\iint \left(\frac{\partial F}{\partial t} + v \frac{\partial F}{\partial x}\right) dv \, dI = \int \left(\frac{\partial \tilde{F}}{\partial t} + v \frac{\partial \tilde{F}}{\partial x}\right) dv = 0$$

we find equation (19) yields

$$\begin{aligned} \iint \beta I \left(\frac{\partial F}{\partial t} + v \frac{\partial F}{\partial x}\right) dv \, dI = &- \frac{3-\gamma}{4(\gamma-1)} \int \\ &\times \left[\frac{\partial}{\partial t} (\tilde{F} \ln \beta)\right. \\ &\left. + v \frac{\partial}{\partial x} (\tilde{F} \ln \beta)\right] dv \\ = &- \frac{3-\gamma}{4(\gamma-1)} \iint \\ &\times \left[\frac{\partial}{\partial t} (F \ln \beta)\right. \\ &\left. + v \frac{\partial}{\partial x} (F \ln \beta)\right] dv \, dI \end{aligned} \tag{20}$$

With equation (20), equation (17) gives

$$\begin{aligned} \frac{\partial H}{\partial t} + \frac{\partial H_v}{\partial x} = &\iint \left(1 + \ln F - \frac{10-6\gamma}{3-\gamma} \beta I\right) \\ &\times \left(\frac{\partial F}{\partial t} + v \frac{\partial F}{\partial x}\right) dv \, dI \end{aligned} \tag{21}$$

If we observe that

$$\begin{aligned} \ln F - \frac{10-6\gamma}{3-\gamma} \beta I = &\left(\ln \rho + \frac{3}{2} \ln \beta + \ln \frac{4(\gamma-1)}{\pi^{1/2}(3-\gamma)} - \beta u^2\right) \\ &+ 2\beta u v - 2\beta \left(I + \frac{v^2}{2}\right) \end{aligned} \tag{22}$$

is the linear combination of collisional invariants 1, v, and $I + \frac{v^2}{2}$ and further that the Euler equations of motion can be cast as

$$\iint \psi \left(\frac{\partial F}{\partial t} + v \frac{\partial F}{\partial x}\right) dv \, dI = 0 \qquad \left(\psi = 1, \; v, \; I + \frac{v^2}{2}\right) \tag{23}$$

equation (21) reduces to the entropy conservation

$$\frac{\partial H}{\partial t} + \frac{\partial H_v}{\partial x} = 0 \tag{24}$$

Thus, every smooth solution of the Euler equations satisfies the entropy conservation equation (24). We will now demonstrate that H decreases during the collision phase in conformity with the H-theorem.

During the collision phase the distribution function suddenly relaxes to F^{n+1} from $f^{\overline{n+1}} = f^n(x - v \, \Delta t)$. Hence, the jump in H during the collision phase is given by

$$\begin{aligned} H^{\overline{n+1}} - H^{n+1} = &\iint \left(f^{\overline{n+1}} \ln f^{\overline{n+1}} - F^{n+1} \ln F^{n+1}\right) dv \, dI \\ &+ \kappa \iint \left(f^{\overline{n+1}} \ln \beta^{\overline{n+1}}\right. \\ &\left. - F^{n+1} \ln \beta^{n+1}\right) dv \, dI \end{aligned} \tag{25}$$

where $\kappa = \frac{5-3\gamma}{2(\gamma-1)}$ and $\beta^{\overline{n+1}} = \beta^n(x - v\,\Delta t)$. Considering the first term on the right-hand side of equation (25), we have

$$\begin{aligned}
&\iint \left(f^{\overline{n+1}} \ln f^{\overline{n+1}} - F^{n+1} \ln F^{n+1}\right) dv\,dI \\
&= \iint f^{\overline{n+1}} \ln \frac{f^{\overline{n+1}}}{F^{n+1}} dv\,dI \\
&\quad + \iint \left(f^{\overline{n+1}} - F^{n+1}\right) \ln F^{n+1}\, dv\,dI \\
&= \iint f^{\overline{n+1}} \ln \frac{f^{\overline{n+1}}}{F^{n+1}} dv\,dI + \frac{10-6\gamma}{3-\gamma} \\
&\quad \times \iint \beta^{n+1} I \left(f^{\overline{n+1}} - F^{n+1}\right) dv\,dI \\
&= \iint f^{\overline{n+1}} \ln \frac{f^{\overline{n+1}}}{F^{n+1}} dv\,dI \\
&\quad + \frac{10-6\gamma}{3-\gamma} \int \beta^{n+1} \left(I_o^{\overline{n+1}} \tilde{f}^{\overline{n+1}} - I_o^{n+1} \tilde{F}^{n+1}\right) dv
\end{aligned} \tag{26}$$

where $\tilde{f}^{\overline{n+1}}$ and $\tilde{F}^{n+1}$ are contracted distributions. Through substitution for I_o, the right-hand side of equation (26) becomes

$$\iint f^{\overline{n+1}} \ln \frac{f^{\overline{n+1}}}{F^{n+1}} dv\,dI + \kappa \int \left(\frac{\beta^{n+1}}{\overline{\beta^{n+1}}} \tilde{f}^{\overline{n+1}} - \tilde{F}^{n+1}\right) dv$$

Noting that

$$\begin{aligned}
\rho^{n+1} &= \iint F^{n+1}\, dv\,dI = \int \tilde{F}^{n+1}\, dv = \iint f^{\overline{n+1}}\, dv\,dI \\
&= \int \tilde{f}^{\overline{n+1}}\, dv
\end{aligned}$$

we obtain

$$\begin{aligned}
&\iint \left(f^{\overline{n+1}} \ln f^{\overline{n+1}} - F^{n+1} \ln F^{n+1}\right) dv\,dI \\
&= \iint f^{\overline{n+1}} \ln \frac{f^{\overline{n+1}}}{F^{n+1}} dv\,dI \\
&\quad + \kappa \iint f^{\overline{n+1}} \left(\frac{\beta^{n+1}}{\overline{\beta^{n+1}}} - 1\right) dv\,dI
\end{aligned} \tag{27}$$

For the second term on the right-hand side of equation (25), we have

$$\begin{aligned}
&\kappa \iint \left(f^{\overline{n+1}} \ln \beta^{\overline{n+1}} - F^{n+1} \ln \beta^{n+1}\right) dv\,dI \\
&= \kappa \iint f^{\overline{n+1}} \ln \frac{\beta^{\overline{n+1}}}{\beta^{n+1}} dv\,dI \\
&\quad + \kappa \iint \ln \beta^{n+1} \left(f^{\overline{n+1}} - F^{n+1}\right) dv\,dI \\
&= \kappa \iint f^{\overline{n+1}} \ln \frac{\beta^{\overline{n+1}}}{\beta^{n+1}} dv\,dI
\end{aligned} \tag{28}$$

because of equation (10). Equations (25), (27), and (28) finally yield

$$\begin{aligned}
H^{\overline{n+1}} - H^{n+1} &= \iint f^{\overline{n+1}} \ln \frac{f^{\overline{n+1}}}{F^{n+1}} dv\,dI \\
&\quad + \kappa \iint f^{\overline{n+1}} \left(\frac{\beta^{n+1}}{\overline{\beta^{n+1}}} \right. \\
&\quad \left. - 1 - \ln \frac{\beta^{n+1}}{\overline{\beta^{n+1}}}\right) dv\,dI
\end{aligned} \tag{29}$$

The second term on the right-hand side of equation (29) is positive because of the inequality

$$x - 1 \geq \ln x \quad , \quad (x > 0) \tag{30}$$

The first term can be shown to be positive by proceeding as follows. We have

$$\begin{aligned}
\iint f^{\overline{n+1}} \ln \frac{F^{n+1}}{\overline{f^{n+1}}} dv\,dI &\leq \iint f^{\overline{n+1}} \left(\frac{F^{n+1}}{\overline{f^{n+1}}} - 1\right) dv\,dI \\
&\leq \iint \left(F^{n+1} - f^{\overline{n+1}}\right) dv\,dI \\
&\leq 0
\end{aligned}$$

because of equation (10). Hence,

$$\iint f^{\overline{n+1}} \ln \frac{f^{\overline{n+1}}}{F^{n+1}} dv\,dI = -\iint f^{\overline{n+1}} \ln \frac{F^{n+1}}{\overline{f^{n+1}}} dv\,dI \geq 0 \tag{31}$$

According to Kullback (ref. 10), the right-hand side of equation (31) is the information theoretic distance between two distributions $f^{\overline{n+1}}$ and F^{n+1}. This distance is always positive and vanishes only if $f^{\overline{n+1}} = F^{n+1}$. Combining equations (29) and (31), we determine that the H-function decreases in the collision phase from H^{n+1} to H^{n+1}. This sudden reduction in the H-function is due to the instantaneous relaxation of the velocity distribution function from $F^n(x - v\,\Delta t)$ to F^{n+1}, and is further due to the convexity property of the H-function.

The validity of the TVNI property for the KNM can be established as follows. Let the distribution function at a mesh point j at the nth time step be denoted by F_j^n. Then,

$$f_j^{\overline{n+1}} = (1 - \xi) F_i^n + \xi F_{i+1}^n \qquad (0 \leq \xi \leq 1)$$

which is a special case of the slightly more general interpolation scheme

$$f_j^{\overline{n+1}} = (1 - \epsilon_i)\, F_i^n + \epsilon_i F_{i+1}^n \qquad (0 \leq \epsilon_i \leq 1) \tag{32}$$

Here i is the mesh point such that $x_j - v\,\Delta t$ lies between x_i and x_{i+1}. The variable ϵ_i can depend on the particle velocity v. The total variation of f is defined by

$$\mathrm{TV}(f^n) = \sum_{\text{all } j} |f^n_{j+1} - f^n_j| = \sum_{\text{all } j} |F^n_{j+1} - F^n_j| \quad (33)$$

During the collision phase, the density, fluid velocity, and temperature do not change (eq. (10)). Hence,

$$\left.\begin{aligned} \mathrm{TV}\left(\rho^{\overline{n+1}}\right) &= \mathrm{TV}\left(\rho^{n+1}\right) \\ \mathrm{TV}\left(u^{\overline{n+1}}\right) &= \mathrm{TV}\left(u^{n+1}\right) \\ \mathrm{TV}\left(T^{\overline{n+1}}\right) &= \mathrm{TV}\left(T^{n+1}\right) \end{aligned}\right\} \quad (34)$$

Therefore, it is sufficient to deal with the change of total variation during the convection phase only. The total variation of $f^{\overline{n+1}}$ is given by

$$\mathrm{TV}\left(f^{\overline{n+1}}\right) = \sum_{\text{all } j} |f^{\overline{n+1}}_{j+1} - f^{\overline{n+1}}_j| \le \sum_{\text{all } i} |(1-\epsilon_i)|F^n_{i+1} - F^n_i| + \sum_{\text{all } i} \epsilon_{i+1}|F^n_{i+2} - F^n_{i+1}| \quad (35)$$

Evidently,

$$\sum_{\text{all } i} \epsilon_{i+1}|F^n_{i+2} - F^n_{i+1}| = \sum_{\text{all } i} \epsilon_i |F^n_{i+1} - F^n_i|$$

and hence the inequality (35) becomes

$$\mathrm{TV}\left(f^{\overline{n+1}}\right) \le \sum_{\text{all } i} |F^n_{i+1} - F^n_i| \le \mathrm{TV}\left(f^n\right)$$

with the use of equation (33). Thus, for every value of v and I, the total variation of the velocity distribution function is nonincreasing during the convection phase. There are some advantages to considering the TV of f instead of the TV of ρ, u, and T. The vector conservation laws of the Euler type are moments of a single scalar equation for f. This equation being linear and hyperbolic admits the exact solution $f(x - v\,\Delta t)$, which is TV-preserving. It is therefore quite consistent to demand that the numerical solution for f be TV-preserving. Further, the TVNI condition on f leads to a wiggle-free solution for the vector conservation equation. On the other hand, the TVNI condition on each of the vector components ρ, ρu, and ρe is, in general, of dubious physical validity even though it gives wiggle-free solutions. The present approach connects the TVNI property of the linear, hyperbolic equation with the vector conservation law by use of the fact that the law is a moment of the equation. From the above analysis the TVNI property of the KNM hinges upon the interpolation strategy adopted in calculating $F(x - v\,\Delta t)$. This fact will be used later while developing a second-order accurate TVD KNM.

A Second-Order Accurate KNM

It has been mentioned in the *Introduction* that the KNM's of Pullin (ref. 1), Reitz (ref. 2), and Deshpande and Raul (ref. 3) suffer from a major disadvantage in that they have numerical diffusion proportional to the time step. From the physical point of view, such a result is only to be expected because the fluid particles in the KNM are allowed to move over time step Δt before they undergo collisions. The distance traveled between collisions is thus proportional to Δt. From the kinetic theory it then follows that the mean free path, and hence the viscosity, will go like Δt. This is a very large amount of viscosity (as the results shown later will verify). Therefore, a modification in the KNM developed earlier is required that will ensure that the method has higher order numerical viscosity. The analysis of this section shows that it is possible to achieve this aim by the use of the Chapman-Enskog theory. It becomes clear later that the development of the second-order accurate KNM is intimately connected with obtaining higher order numerical viscosity.

For one-dimensional compressible inviscid flow, the governing Euler equations are

$$\left.\begin{aligned} \frac{\partial}{\partial t}(\rho) + \frac{\partial}{\partial x}(\rho u) &= 0 \\ \frac{\partial}{\partial t}(\rho u) + \frac{\partial}{\partial x}(p + \rho u^2) &= 0 \\ \frac{\partial}{\partial t}(\rho e) + \frac{\partial}{\partial x}(\rho u e + p u) &= 0 \end{aligned}\right\} \quad (36)$$

As $D_f = 1$, equations (4) and (5) yield

$$e = I_o + \frac{RT}{2} + \frac{u^2}{2} = \frac{RT}{\gamma - 1} + \frac{u^2}{2} \quad (37)$$

The second-order accurate Taylor expansions for

$\rho^{n+1}, (\rho u)^{n+1}$, and $(\rho e)^{n+1}$ are

$$\left.\begin{aligned}
\rho^{n+1} &= \rho^n + \left(\frac{\partial \rho}{\partial t}\right)^n \Delta t + \left(\frac{\partial^2 \rho}{\partial t^2}\right) + O(\Delta t^3) \\
(\rho u)^{n+1} &= (\rho u)^n + \left(\frac{\partial}{\partial t}\rho u\right)^n \Delta t \\
&\quad + \left(\frac{\partial^2}{\partial t^2}\rho u\right)^n \frac{\Delta t^2}{2} + O(\Delta t^3) \\
(\rho e)^{n+1} &= (\rho e)^n + \left(\frac{\partial}{\partial t}\rho e\right)^n \Delta t \\
&\quad + \left(\frac{\partial^2}{\partial t^2}\rho e\right)^n \frac{\Delta t^2}{2} + O(\Delta t^3)
\end{aligned}\right\} \quad (38)$$

These expansions contain the first- and second-order time derivatives of ρ, ρu, and ρe. The first-order time derivatives can be replaced in terms of the first-order space derivatives by equations (36). Replacing the second-order time derivatives in terms of the space derivatives requires detailed manipulations, which are shown in appendix B. With the results of appendix B, the Taylor expansions (38) become

$$\rho^{n+1} = \rho^n - \Delta t \frac{\partial}{\partial x}(\rho u)^n + \frac{\Delta t^2}{2}\frac{\partial^2}{\partial x^2}(p + \rho u^2)^n + O(\Delta t^3) \quad (39)$$

$$(\rho u)^{n+1} = (\rho u)^n - \Delta t \frac{\partial}{\partial x}(p + \rho u^2)^n + \frac{\Delta t^2}{2}\frac{\partial^2}{\partial x^2}(3pu + \rho u^3)^n - \frac{\Delta t^2}{2}\frac{\partial}{\partial x}\left[(3-\gamma)p\frac{\partial u}{\partial x}\right]^n + O(\Delta t^3) \quad (40)$$

$$\begin{aligned}
(\rho e)^{n+1} &= (\rho e)^n - \Delta t \frac{\partial}{\partial x}(\rho e u + p u)^n \\
&\quad + \frac{\Delta t^2}{2}\frac{\partial^2}{\partial x^2}\left[\frac{5\gamma - 3}{2(\gamma - 1)}pu^2 + \frac{\gamma}{\gamma - 1}\frac{p^2}{\rho} + \frac{\rho u^4}{2}\right]^n \\
&\quad - \frac{\Delta t^2}{2}\frac{\partial}{\partial x}\left[(3-\gamma)pu\frac{\partial u}{\partial x} + \frac{\gamma}{\gamma - 1}p\frac{\partial}{\partial x}\left(\frac{p}{\rho}\right)\right]^n \\
&\quad + O(\Delta t^3)
\end{aligned} \quad (41)$$

Notice that the local Maxwellian distribution F satisfies the moment equations

$$\left.\begin{aligned}
\int F\, dv\, dI &= \rho \\
\int vF\, dv\, dI &= \rho u \\
\iint v^2 F\, dv\, dI &= p + \rho u^2 \\
\iint \left(I + \frac{v^2}{2}\right) F\, dv\, dI &= \rho e \\
\iint v^3 F\, dv\, dI &= 3pu + \rho u^3 \\
\iint \left(I + \frac{v^2}{2}\right) v^2 F\, dv\, dI &= \frac{5\gamma - 3}{2(\gamma - 1)}pu^2 \\
&\quad + \frac{\gamma}{\gamma - 1}\left(\frac{p^2}{\rho}\right) + \frac{\rho u^4}{2}
\end{aligned}\right\} \quad (42)$$

Through use of the moment equations (42), the Taylor expansions (39), (40), and (41) can be cast as

$$\begin{aligned}
\begin{bmatrix} \rho \\ \rho u \\ \rho e \end{bmatrix}^{n+1} &= \begin{bmatrix} \rho \\ \rho u \\ \rho e \end{bmatrix}^n - \Delta t \frac{\partial}{\partial x}\iint dv\, dI\, vF^n \begin{bmatrix} 1 \\ v^2 \\ I + \frac{v^2}{2} \end{bmatrix} \\
&\quad + \frac{\Delta t^2}{2}\frac{\partial^2}{\partial x^2}\int dv\, dI\, v^2 F^n \begin{bmatrix} 1 \\ v^2 \\ I + \frac{v^2}{2} \end{bmatrix} \\
&\quad - \frac{\partial}{\partial x}\begin{bmatrix} 0 \\ \frac{\Delta t^2}{2}(3-\gamma)p\frac{\partial u}{\partial x} \\ \frac{\Delta t^2}{2}(3-\gamma)pu\frac{\partial u}{\partial x} + \frac{\gamma}{\gamma - 1}p\frac{\partial}{\partial x}\left(\frac{p}{\rho}\right) \end{bmatrix}^n \\
&\quad + O(\Delta t^3)
\end{aligned} \quad (43)$$

From use of the second-order accurate Taylor expansion

$$F^n(x - v\,\Delta t) = F^n - v\,\Delta t\left(\frac{\partial F}{\partial x}\right)^n + \frac{v^2\,\Delta t^2}{2}\left(\frac{\partial^2 F}{\partial x^2}\right)^n + \cdots$$

and with the definitions

$$\begin{aligned}
\tau &= -\frac{\Delta t}{2}(3-\gamma)p\frac{\partial u}{\partial x} \\
q &= -\frac{\Delta t}{2}\frac{\gamma}{\gamma - 1}p\frac{\partial}{\partial x}\left(\frac{p}{\rho}\right)
\end{aligned} \quad (44)$$

the Taylor expansions (43) take on the simple form

$$\begin{aligned}
\begin{bmatrix} \rho \\ \rho u \\ \rho e \end{bmatrix}^{n+1} &= \iint dv\, dI\, F^n(x - v\,\Delta t)\begin{bmatrix} 1 \\ v \\ I + \frac{v^2}{2} \end{bmatrix} \\
&\quad + \Delta t \frac{\partial}{\partial x}\begin{bmatrix} 0 \\ \tau \\ \tau u + q \end{bmatrix} + O(\Delta t^3)
\end{aligned} \quad (45)$$

Equation (45) reveals a very important feature of the KNM. The right-hand side of equation (45) consists of two terms; the first is an upwind term because of the presence of $F^n(x - v\,\Delta t)$, and the second is an antidiffusive term containing τ and q. The antidiffusive nature results because τ and q defined by equation (45) are analogous to negative viscous stress and negative heat flux. To achieve second-order accuracy in both space and time, it is essential to consider both the upwind term and the antidiffusive term. Further, $F(x - v\,\Delta t)$ appearing in the upwind term must be evaluated for second-order accuracy in space by using a suitable interpolation scheme. Note that the antidiffusive term is $O(\Delta t^2)$, and therefore second-order accuracy in space is attained with the use of the upwind term alone if Δt is chosen such that $O(\Delta t) = O\left(\Delta x^{3/2}\right)$. For Courant numbers of the order of unity, the antidiffusive term is $O(\Delta x^2)$. Thus, any version of KNM in which only the upwind term is considered and the Courant number $O(1)$ is used cannot achieve second-order accuracy regardless of the accuracy of the interpolation scheme. This fact has not been noticed in the earlier work. For example, Reitz (ref. 2) ignores the antidiffusive term and uses a second-order accurate interpolation formula for calculating $F(x - v\,\Delta t)$, presumably to achieve second-order accuracy. As the Courant number chosen by him is $O(1)$, it is clear that his calculations are subject to the truncation error $O(\Delta x^2)$ and thus are first-order accurate.

The preceding analysis shows that a modification in the ansatz is necessary for constructing a second-order accurate method. This modified ansatz $f_o = f_o(t, x, v, I)$ must satisfy the constraints

$$\begin{aligned}\iint \begin{bmatrix} 1 \\ v \\ I + \frac{v_2}{2} \end{bmatrix} f_o(t, x - v\,\Delta t, v, I)\,dv\,dI \\ = \iint \begin{bmatrix} 1 \\ v \\ I + \frac{v_2}{2} \end{bmatrix} F(t, x - v\,\Delta t, v, I)\,dv\,dI \\ + \frac{\partial}{\partial x} \begin{bmatrix} 0 \\ \tau\,\Delta t \\ (\tau u + q)\Delta t \end{bmatrix} + O(\Delta t^3) \end{aligned} \tag{46}$$

These constraints are satisfied if

$$\iint \begin{bmatrix} 1 \\ v \\ I + \frac{v_2}{2} \end{bmatrix} (f_o - F)\,dv\,dI = O\left(\Delta t^3\right) \tag{47}$$

$$\iint \begin{bmatrix} 1 \\ v \\ I + \frac{v_2}{2} \end{bmatrix} v(f_o - F)\,dv\,dI = \begin{bmatrix} 0 \\ \tau \\ (\tau u + q) \end{bmatrix} + O\left(\Delta t^2\right) \tag{48}$$

$$\iint \begin{bmatrix} 1 \\ v \\ I + \frac{v_2}{2} \end{bmatrix} v^2 (f_o - F)\,dv\,dI = O(\Delta t) \tag{49}$$

The conditions in equation (47) merely state that the density, velocity, and energy for f_o and F must be identical within the truncation error. They are therefore conservation conditions. With the definitions in equations (4) for viscous stress and heat flux, the conditions in equation (48) can be equivalently cast as

$$\iint (v - u)^2 f_o\,dv\,dI = p - \tau \tag{50}$$

$$\iint \left[I + \frac{(v - u)^2}{2}\right](v - u) f_o = -q \tag{51}$$

Equations (50) and (51) require that the distribution function f_o must have nonvanishing viscous stress and heat flux. They therefore suggest the use of the Chapman-Enskog distribution instead of the Maxwellian distribution. This is further supported by the observation that equation (43), which is the basis of equation (46), is obtained by replacing the time derivatives of field variables with their space derivatives using Euler equations. Such a replacement is very characteristic of the Chapman-Enskog analysis.

Consider the model Boltzmann equation

$$\frac{\partial f}{\partial t} + v\frac{\partial f}{\partial x} = \alpha(F - f) \tag{52}$$

where α is a time constant characteristic of collisions. The parameter α may depend on space but is independent of v and I. For large values of α it is advantageous to write equation (52) in the form

$$\begin{aligned} f &= F - \frac{1}{\alpha}\left(\frac{\partial f}{\partial t} + v\frac{\partial f}{\partial x}\right) \\ &= F - \frac{1}{\alpha}\left(\frac{\partial F}{\partial t} + v\frac{\partial F}{\partial x}\right) + O\left(\alpha^{-2}\right) \end{aligned} \tag{53}$$

The Chapman-Enskog distribution is given by

$$f_{\mathrm{CE}} = F - \frac{1}{\alpha}\left(\frac{\partial F}{\partial t} + v\frac{\partial F}{\partial x}\right)$$

With the results of appendix C, the above distribution can be written as

$$f_{\mathrm{CE}} = F\left[1 - \frac{\tau_{\mathrm{CE}}}{p}P_\tau(v, I) - \frac{q_{\mathrm{CE}}}{p(2RT)^{1/2}}P_q(v, I)\right] \tag{54}$$

where

$$\left.\begin{aligned} \tau_{CE} &= \frac{3-\gamma}{\alpha} p \frac{\partial u}{\partial x} \\ q_{CE} &= \frac{\gamma}{\alpha(\gamma-1)} p \frac{\partial}{\partial x}\left(\frac{p}{\rho}\right) \end{aligned}\right\} \tag{55}$$

$$P_\tau = \frac{3\gamma-5}{2(3-\gamma)} - \frac{4(\gamma-1)^2}{3-\gamma}\frac{I}{2RT} + C^2 \tag{56}$$

$$P_q = \frac{2(\gamma-1)}{\gamma}\left[-\frac{5C}{2} + C^3 + \frac{4(\gamma-1)}{3-\gamma} C \frac{I}{2RT}\right] \tag{57}$$

$$C = \frac{v-u}{(2RT)^{1/2}}$$

Equations (55) and (44) immediately fix α at $\alpha = -\frac{2}{\Delta t}$. The model equation (52) then becomes

$$\frac{\partial f}{\partial t} + v\frac{\partial f}{\partial x} = -\frac{2}{\Delta t}(F - f)$$

The characteristic collision time for this equation is half the time step Δt, and this result merely confirms the earlier argument about the numerical diffusion being proportional to Δt. The sign of α is negative because the numerical diffusion inherent in the first-order KNM has to be cancelled to develop a second-order KNM. Thus, the Chapman-Enskog terms in equation (54) are antidiffusive. That f_{CE} defined by equation (54) is the required distribution can be clearly seen from the following relations:

$$\iint \begin{bmatrix} 1 \\ v \\ I + \frac{v^2}{2} \end{bmatrix} (f_{CE} - F)\, dv\, dI = 0$$

$$\iint (v-u)^2 f_{CE}\, dv\, dI = p - \tau_{CE}$$

$$\iint \left[I + \frac{(v-u)^2}{2}\right](v-u) f_{CE}\, dv\, dI = -q_{CE}$$

$$\iint \begin{bmatrix} 1 \\ v \\ I + \frac{v^2}{2} \end{bmatrix} v^2 (f_{CE} - F)\, dv\, dI = O(\Delta t)$$

These moment equations can be easily derived by integrating f_{CE}. They are identical with the conditions (47), (48), and (49). It therefore follows that a second-order accurate solution in time is given by

$$\begin{bmatrix} \rho \\ \rho u \\ \rho e \end{bmatrix}^{n+1} = \iint \begin{bmatrix} 1 \\ v \\ I + \frac{v^2}{2} \end{bmatrix} f_{CE}^n(x - v\,\Delta t, v, I)\, dv\, dI + O\left(\Delta t^3\right) \tag{58}$$

Several important features of the above second-order accurate KNM are worth noting. Equation (58), containing the Chapman-Enskog distribution, has been derived from equation (45). As stated previously, the right-hand side of equation (45) contains two terms. The first term, which is a moment of $F^n(x - v\,\Delta t)$, is upwind in character. The second term cannot be expressed as a moment of $F^n(x - v\,\Delta t)$ and is antidiffusive. The antidiffusive term may be absorbed in the upwind term only if the distribution function is not Maxwellian. Equation (58) is an upwind version of a second-order accurate solution in which the perturbed Maxwellian distribution or, equivalently, the Chapman-Enskog distribution is employed. Obviously, τ_{CE} and q_{CE} of the Chapman-Enskog distribution f_{CE} are antidiffusive. Furthermore, because of the presence of τ_{CE} and q_{CE}, the Chapman-Enskog distribution not only depends on local values of field variables but also depends on their neighboring values as well. The support of the Chapman-Enskog distribution is thus more than that of the local Maxwellian distribution used in first-order accurate KNM.

The Chapman-Enskog distribution function f_{CE} can assume physically meaningless negative values for sufficiently large values of velocity v. From equation (54) it is obvious that f_{CE} can become negative if

$$\left|\frac{q_{CE}}{p(2RT)^{1/2}}\right| v^3 = O(1) \tag{59}$$

that is, if $v > O\left(\Delta t^{-1/3}\right)$. As Narasimha (ref. 11) has noted, the Chapman-Enskog distribution is only an inner solution in v-space and is not valid for relatively high velocities. It is possible to modify the Chapman-Enskog distribution along the lines of Narasimha's analysis (ref. 11).

Another important point about equation (58) is that $f_{CE}(x_j - v\,\Delta t)$ needs to be evaluated at various values of v. Hence, as noted before, some kind of interpolation scheme is required. This scheme must be second-order accurate in space, should yield non-negative interpolated values, and should satisfy the TVNI sufficiency condition of equation (32). These questions are addressed in a subsequent section.

Interpolation Scheme

The central problem in devising an interpolation scheme is to evaluate $f(x_j - v\,\Delta t)$, given the values of f at mesh points, so that the conditions set forth previously are satisfied. Let the mesh point i corresponding to point j be such that

$$x_j - v\,\Delta t = x_i + \xi\,\Delta x \qquad (0 \le \xi \le 1) \tag{60}$$

The function $f(x_j - v\,\Delta t) = f(x_i + \xi\,\Delta x)$ then depends on the neighboring mesh points $i \pm 1$. In fact, the Taylor expansion yields

$$f(x_i + \xi\,\Delta x) = f_i + \frac{\xi}{2}\left(f_{i+1} - f_{i-1}\right) + \frac{\xi^2}{2}\left(f_{i+1} - 2f_i + f_{i-1}\right)$$

Unfortunately, the above expansion does not automatically ensure positivity of $f(x_i + \xi\,\Delta x)$ even if f_i and $f_{i\pm1}$ are assumed to be positive. This is particularly true for calculations near shocks. To devise the desired interpolation formula, first write the above Taylor expansion equivalently as

$$f(x_i + \xi\,\Delta x) = (1-\xi)f_i + \xi f_{i+1} - \frac{\xi(1-\xi)}{2}\left(f_{i+1} - 2f_i + f_{i-1}\right) \tag{61}$$

Now,

$$\begin{aligned}
&\frac{\xi(1-\xi)}{2}\left(f_{i+1} - 2f_i + f_{i-1}\right) \\
&= \frac{\xi(1-\xi)^2}{2}\left(f_{i+1} - 2f_i + f_{i-1}\right) \\
&\quad + \frac{\xi^2(1-\xi)}{2}\left(f_{i+1} - 2f_i + f_{i-1}\right) \\
&= 2\xi(1-\xi)^2\frac{f_{i+1} - 2f_i + f_{i-1}}{f_{i+1} - 2f_i + f_{i-1}}f_i \\
&\quad + 2\xi^2(1-\xi)\frac{f_{i+1} - 2f_i + f_{i-1}}{f_{i+1} + 2f_i + f_{i-1}}f_{i+1} + O(\Delta x^3) \\
&= 2\xi(1-\xi)\phi_i\left[(1-\xi)f_i + \xi f_{i+1}\right] + O(\Delta x^3)
\end{aligned}$$

where

$$\phi_i = \frac{f_{i+1} - 2f_i + f_{i-1}}{f_{i+1} + 2f_i + f_{i-1}}$$

The function ϕ_i has the property $|\phi_i| \le 1$ if f_i and $f_{i\pm1}$ are positive. In terms of ϕ_i, the interpolation formula (eq. (61)) becomes

$$f(x_i + \xi\,\Delta x) = \left[(1-\xi)f_i + \xi f_{i+1}\right]\left[1 - 2\xi(1-\xi)\phi_i\right] \tag{62}$$

Because $|2\xi(1-\xi)\phi_i| \le 1$ if f_i and $f_{i\pm1}$ are positive, it follows that equation (62) yields only positive interpolated values as long as the distribution function is positive. Unfortunately, equation (62) does not satisfy the TVNI sufficiency condition. This is because ϕ_i can become negative, and in that case,

$$1 - 2\xi(1-\xi)\phi_i = 1 + 2\xi(1-\xi)|\phi_i| > 1$$

It is not possible then to write equation (62) in the form

$$f(x_i + \xi\,\Delta x) = \epsilon_i f_i + \epsilon_i' f_{i+1}$$

with the constraints $0 \le \epsilon_i \le 1, 0 \le \epsilon_i \le 1$, and $\epsilon_i + \epsilon_i' \le 1$. With the method of Chakravarthy and Osher (ref. 12) limiting the contribution of the second difference, it is possible to devise an interpolation scheme that satisfies the TVNI sufficiency condition.

The second-order accurate Taylor expansion can be written as

$$\begin{aligned}
f(x_i + \xi\,\Delta x) &= f_i + \frac{\xi}{2}\left(f_{i+1} - f_i + f_i - f_{i-1}\right) \\
&\quad + \frac{\xi^2}{2}\left(f_{i+1} - f_i + f_{i-1} - f_i\right) \\
&= f_i + \frac{\xi(1+\xi)}{2}\left(f_{i+1} - f_i\right) \\
&\quad + \frac{\xi(1-\xi)}{2}\left(f_i - f_{i-1}\right) \\
&= f_i + \left(f_{i+1} - f_i\right)\left[\frac{\xi(1+\xi)}{2}\right. \\
&\quad \left. + \frac{\xi(1-\xi)}{2}r_D\right]
\end{aligned} \tag{63}$$

where

$$r_D = \frac{\text{Backward difference}}{\text{Forward difference}} = \frac{f_i - f_{i-1}}{f_{i+1} - f_i} \tag{64}$$

In smooth regions,

$$r_D = 1 - \Delta x\frac{f_i''}{f_i'} + O(\Delta x^2)$$

and thus r_D remains close to unity. In flow regions near shocks or contact surfaces, r_D can wildly vary and some limiting criterion is required to preserve the TVNI condition. The key to satisfying the TVNI condition lies in requiring

$$0 \le \frac{\xi(1+\xi)}{2} + \frac{\xi(1-\xi)}{2}r_D \le 1 \tag{65}$$

Two cases arise, namely, $r_D \ge 0$ and $r_D \le 0$. If we consider the case of $r_D \ge 0$, the condition in equation (65) is satisfied if

$$r_D \le 1 + \frac{2}{\xi} \tag{66}$$

As $0 \le \xi \le 1$, the right-hand side of the above inequality has the minimum value of 3. One way of satisfying equation (66) is to limit the value of r_D to 3 when $r_D \ge 0$. For the case when $r_D \le 0$, the condition in equation (65) is satisfied if

$$\frac{\xi(1+\xi)}{2} + \frac{\xi(1-\xi)}{2}r_D = \frac{\xi(1+\xi)}{2} - \frac{\xi(1-\xi)}{2}|r_D| \ge 0$$

or, equivalently, if

$$|r_D| \le \frac{1+\xi}{1-\xi} \tag{67}$$

Thus, by limiting the relative values of the forward and backward differences and taking $r_D = 1$ outside these limits, we find the interpolation formula in equation (63) yields not only positive values of $f(x_i + \xi\,\Delta x)$ but also satisfies the TVNI condition. As mentioned previously, the basic input to equation (63) is the set of positive values of f_i at all mesh points.

From the analysis in previous sections it has become clear that the second-order accurate KNM requires the use of the Chapman-Enskog distribution and a second-order accurate interpolation scheme. The development of the KNM so far has been restricted to one-dimensional unsteady, inviscid compressible flows. The extension of the KNM to two-dimensional steady supersonic flow is considered in the next section.

Extension of the KNM to Two-Dimensional Steady Supersonic Flow

So far, the development of the kinetic numerical method (KNM) for the unsteady Euler equations has been considered. The steady Euler equations for supersonic flow are hyperbolic, and hence a space-marching version of the KNM can be developed along similar lines. In this section, various steps involved in developing the Euler space-marching KNM are given.

The two-dimensional steady Euler equations are

$$\left.\begin{aligned}
&\frac{\partial}{\partial x_1}(\rho u_1) + \frac{\partial}{\partial x_2}(\rho u_2) = 0\\
&\frac{\partial}{\partial x_1}\left(p + \rho u_1^2\right) + \frac{\partial}{\partial x_2}(\rho u_1 u_2) = 0\\
&\frac{\partial}{\partial x_1}(\rho u_1 u_2) + \frac{\partial}{\partial x_2}\left(p + \rho u_2^2\right) = 0\\
&\frac{\partial}{\partial x_1}(\rho e u_1 + p u_1) + \frac{\partial}{\partial x_2}(\rho e u_2 + p u_2) = 0
\end{aligned}\right\} \tag{68}$$

where $e = \frac{p}{\rho(\gamma-1)} + \frac{u_1^2 + u_2^2}{2}$.

Equations (68) can be obtained as the moments of the steady Boltzmann equation

$$v_1\frac{\partial f}{\partial x_1} + v_2\frac{\partial f}{\partial x_2} = J(f,f) \tag{69}$$

if the velocity distribution function f is Maxwellian:

$$F = \frac{\rho}{2\pi RT I_o}\exp\left[-\frac{(v_1-u_1)^2 + (v_2-u_2)^2}{2RT} - \frac{I}{I_o}\right] \tag{70}$$

where $I_o = \frac{2-\gamma}{\gamma-1}RT$. The field variables ρ, u, and T are related to f through the moment equations

$$\left.\begin{aligned}
\rho &= \iiint f\,dv_1\,dv_2\,dI\\
\rho\mathbf{u} &= \iiint \mathbf{v} f\,dv_1\,dv_2\,dI\\
\rho e &= \iiint \left(I + \frac{v^2}{2}\right) f\,dv_1\,dv_2\,dI
\end{aligned}\right\} \tag{71}$$

The KNM for equations (68) can be constructed by splitting the Boltzmann equation (69) as follows:

$$v_1\frac{\partial f}{\partial x_1} + v_2\frac{\partial f}{\partial x_2} = 0 \tag{72}$$

$$J(f,f) = 0 \tag{73}$$

The exact solution of equation (72) is given by

$$f(x_1 + \Delta x_1, x_2, v_1, v_2, I) = f(x_1, x_2 - \tilde{c}\,\Delta x_1, \Delta x_1, v_2, I) \tag{74}$$

where $\tilde{c} = \frac{v_2}{v_1}$. In the convection phase, therefore, the fluid particles at $x_1 + \Delta x_1$ and x_2 come from x_1 and $x_2 - \tilde{c}\,\Delta x_1$. The collision phase, governed by equation (73), merely says that the distribution function f is a local Maxwellian distribution everywhere.

Consider a two-dimensional mesh of points (n, j) within a rectangular computational domain. The index n is along the X_1-axis and the index j is along the X_2-axis. Because x_1 is a time-like coordinate in the integration of the hyperbolic equation (72), the finite-difference solution for the line $n+1$ can be obtained from the data for the line n. We introduce the following notation:

$$f^n = f(n\,\Delta x_1,\ x_2,\ v_1,\ v_2,\ I) = f(n\,\Delta x_1,\ x_2)$$

The solution (74) can then be written as

$$f_j^{n+1} = f\left(n\,\Delta x_1,\ x_{2j} - \tilde{c}\,\Delta x_1\right) \tag{75}$$

$$(\rho u_1)^{n+1} = \iiint v_1 f\left(n\,\Delta x_1,\ x_{2j} - \tilde{c}\,\Delta x_1\right) dv_1\,dv_2\,dI \tag{76}$$

$$\left(p + \rho u_1^2\right)_j^{n+1} = \iiint v_1^2 f\left(n\,\Delta x_1, x_{2j} - \tilde{c}\,\Delta x_1\right) dv_1\,dv_2\,dI \tag{77}$$

$$(\rho u_1 u_2)_j^{n+1} = \iiint v_1 v_2 f\left(n\,\Delta x_1, x_{2j} - \tilde{c}\,\Delta x_1\right) dv_1\,dv_2\,dI \tag{78}$$

$$(\rho e u_1 + p u_1)_j^{n+1} = \iiint v_1\left(I + \frac{v^2}{2}\right) \times f\left(n\,\Delta x_1, x_{2j} - \tilde{c}\,\Delta x_1\right) dv_1\,dv_2\,dI \tag{79}$$

Note that because of equation (73) the velocity distribution f is the Maxwellian distribution in equation (70). The moment function $\boldsymbol{\Psi}$ is defined as

$$\boldsymbol{\Psi} = \left[v_1, v_1^2, v_1 v_2, v_1\left(I + \frac{v^2}{2}\right)\right]^T \tag{80}$$

and the inner product is defined by

$$\langle \boldsymbol{\Psi}, F\rangle = \iiint \psi F(v, I) dv_1\, dv_2\, dI$$

with suitable limits for v_1, v_2, and I. Equations (76) to (79) can then be written in the following compressed notation:

$$\left\langle \boldsymbol{\Psi}, F_j^{n+1}\right\rangle = \left\langle \boldsymbol{\Psi}, F\left(x_{1_n}, x_{2_j} - \tilde{c}\,\Delta x_1, I\right)\right\rangle \tag{81}$$

which is obtained by taking the $\boldsymbol{\Psi}$-moment of equation (75). The KNM space-marching scheme for the Euler equations (68) is therefore simply the $\boldsymbol{\Psi}$-moment of the exact solution of the collisionless Boltzmann equation (72). The KNM space-marching scheme in equation (81) is first-order accurate in x_1 and x_2.

For the purpose of developing a second-order accurate Euler space-marching scheme, we first note that

$$\langle \boldsymbol{\Psi}, F(x_1 + \Delta x_1, x_2)\rangle = \langle \boldsymbol{\Psi}, F\rangle + \Delta x_1\left\langle \boldsymbol{\Psi}, \frac{\partial F}{\partial x_1}\right\rangle + \frac{\Delta x_1^2}{2}\left\langle \boldsymbol{\Psi}, \frac{\partial^2 F}{\partial x_1^2}\right\rangle + O\left(\Delta x_1^3\right) \tag{82}$$

The $\boldsymbol{\Psi}$-moment of the collisionless Boltzmann equation (72) yields

$$\left\langle \boldsymbol{\Psi}, \frac{\partial F}{\partial x_1}\right\rangle = -\left\langle \boldsymbol{\Psi}, \tilde{c}\frac{\partial F}{\partial x_2}\right\rangle \tag{83}$$

Combining equations (82) and (83) gives

$$\langle \boldsymbol{\Psi}, F(x_1 + \Delta x_1, x_2)\rangle = \langle \boldsymbol{\Psi}, F\rangle - \Delta x_1\left\langle \boldsymbol{\Psi}, \tilde{c}\frac{\partial F}{\partial x_2}\right\rangle + \frac{\Delta x_1^2}{2}\left\langle \boldsymbol{\Psi}, \frac{\partial^2 F}{\partial x_1^2}\right\rangle + O\left(\Delta x_1^3\right) \tag{84}$$

From equation (84) it is obvious that to develop a second-order accurate KNM, the second partial derivative of F with respect to x_1 must be obtained in terms of its derivatives with respect to x_2. For this purpose, we proceed as follows. Let

$$\frac{\partial F}{\partial x_1} + \tilde{c}\frac{\partial F}{\partial x_2} = P_{\mathrm{CE}} F \tag{85}$$

Thus, $P_{\mathrm{CE}} = \frac{\partial}{\partial x_1}(\ln F) + \tilde{c}\frac{\partial}{\partial x_2}(\ln F)$. Replacing RT in equation (70) by $\frac{p}{\rho}$, we get

$$F = \frac{\rho^3(\gamma - 1)}{2\pi p^2(2-\gamma)} \times \exp\left[-\frac{\rho(v_1 - u_1)^2 + \rho(v_2 - u_2)^2}{2p} - \frac{\rho I}{p}\frac{\gamma - 1}{2 - \gamma}\right]$$

which gives

$$\ln F = 3\ln\rho - 2\ln p - \frac{\rho I}{p}\frac{\gamma - 1}{2-\gamma} - \frac{\rho(v_1 - u_1)^2 + \rho(v_2 - u_2)^2}{2p} + \ln\frac{\gamma - 1}{2\pi(2-\gamma)}$$

Hence,

$$\begin{aligned}\left(\frac{\partial}{\partial x_1} + \tilde{c}\frac{\partial}{\partial x_2}\right)\ln F = {} & \left(\frac{\partial \rho}{\partial x_1} + \tilde{c}\frac{\partial \rho}{\partial x_2}\right) \\ & \times \left[\frac{3}{\rho} - \frac{(v_1 - u_1)^2 + (v_2 - u_2)^2}{2p} - \frac{I}{p}\frac{\gamma - 1}{2 - \gamma}\right] \\ & + \left(\frac{\partial u_1}{\partial x_1} + \tilde{c}\frac{\partial u_1}{\partial x_2}\right)\frac{\rho(v_1 - u_1)}{p} \\ & + \left(\frac{\partial u_2}{\partial x_1} + \tilde{c}\frac{\partial u_2}{\partial x_2}\right)\frac{\rho(v_2 - u_2)}{p} \\ & + \left(\frac{\partial p}{\partial x_1} + \tilde{c}\frac{\partial p}{\partial x_2}\right) \\ & \times \left[-\frac{2}{p} + \frac{\rho(v_1 - u_1)^2 + \rho(v_2 - u_2)^2}{2p^2} + \frac{\rho I}{p^2}\frac{\gamma - 1}{2 - \gamma}\right]\end{aligned}$$

After a little manipulation we obtain

$$\begin{aligned}P_{\mathrm{CE}} = {} & \left(\frac{\partial}{\partial x_1} + \tilde{c}\frac{\partial}{\partial x_2}\right)\ln F \\ = {} & \frac{1}{\rho}\left(\frac{\partial \rho}{\partial x_1} + \tilde{c}\frac{\partial \rho}{\partial x_2}\right) \\ & \times \left[3 - \frac{(v_1 - u_1)^2 + (v_2 - u_2)^2}{2RT} - \frac{\gamma - 1}{2 - \gamma}\frac{I}{RT}\right] \\ & + \left(\frac{\partial u_1}{\partial x_1} + \tilde{c}\frac{\partial u_1}{\partial x_2}\right)\frac{v_1 - u_1}{RT} + \left(\frac{\partial u_2}{\partial x_1} + \tilde{c}\frac{\partial u_2}{\partial x_2}\right)\frac{v_2 - u_2}{RT} \\ & + \frac{1}{p}\left(\frac{\partial p}{\partial x_1} + \tilde{c}\frac{\partial p}{\partial x_2}\right) \\ & \times \left[\frac{I}{RT}\frac{\gamma - 1}{2 - \gamma} + \frac{(v_1 - u_1)^2 + (v_2 - u_2)^2}{2RT} - 2\right]\end{aligned} \tag{86}$$

The function P_{CE} is a polynomial in $\tilde{c}$, v_1, and I. This is evident after replacing v_2 by $\tilde{c}v_1$. The space derivatives of ρ, u_1, u_2, and p with respect to x_1 can

be replaced by x_2 space derivatives from the Euler equations. (See appendix D.) Now

$$\begin{aligned}\frac{\partial^2 F}{\partial x_1^2} &= -\frac{\partial}{\partial x_1}\left(\tilde{c}\frac{\partial F}{\partial x_2}\right) + \frac{\partial}{\partial x_1}(P_{\mathrm{CE}}F) \\ &= -\frac{\partial}{\partial x_2}\left(\tilde{c}\frac{\partial F}{\partial x_1}\right) + \frac{\partial}{\partial x_1}(P_{CE}F) \\ &= -\frac{\partial}{\partial x_2}\left(-\tilde{c}^2\frac{\partial F}{\partial x_2} + \tilde{c}P_{\mathrm{CE}}F\right) + \frac{\partial}{\partial x_1}(P_{\mathrm{CE}}F) \\ &= \tilde{c}^2\frac{\partial^2 F}{\partial x_2^2} - \tilde{c}\frac{\partial}{\partial x_2}(P_{\mathrm{CE}}F) + \frac{\partial}{\partial x_1}(P_{\mathrm{CE}}F) \qquad (87)\end{aligned}$$

Notice that

$$\begin{aligned}\left\langle \Psi, \frac{\partial}{\partial x_1}(P_{\mathrm{CE}}F)\right\rangle &= \frac{\partial}{\partial x_1}\left\langle \Psi, P_{\mathrm{CE}}F\right\rangle \\ &= \frac{\partial}{\partial x_1}\left\langle \Psi, \frac{\partial F}{\partial x_1} + \tilde{c}\frac{\partial F}{\partial x_2}\right\rangle \\ &= 0\end{aligned}$$

This is because

$$\left\langle \Psi, \frac{\partial F}{\partial x_1} + \tilde{c}\frac{\partial F}{\partial x_2}\right\rangle = 0$$

represents the Euler equations. Therefore,

$$\left\langle \Psi, \frac{\partial^2 F}{\partial x_1^2}\right\rangle = \left\langle \Psi, \tilde{c}^2\frac{\partial^2 F}{\partial x_2^2}\right\rangle - \left\langle \Psi, \tilde{c}\frac{\partial}{\partial x_2}(P_{\mathrm{CE}}F)\right\rangle \qquad (88)$$

Substitution for $\left\langle \Psi, \frac{\partial^2 F}{\partial x_1^2}\right\rangle$ in equation (84) finally gives

$$\begin{aligned}\langle \Psi, F(x_1+\Delta x_1, x_2)\rangle = &\langle \Psi, F\rangle - \Delta x_1\left\langle \Psi, \tilde{c}\frac{\partial F}{\partial x_2}\right\rangle \\ &+ \frac{\Delta x_1^2}{2}\left\langle \Psi, \tilde{c}^2\frac{\partial^2 F}{\partial x_2^2}\right\rangle \\ &- \frac{\Delta x_1^2}{2}\left\langle \Psi, \tilde{c}\frac{\partial}{\partial x_2}(P_{\mathrm{CE}}F)\right\rangle \\ &+ O\left(\Delta x_1^3\right) \qquad (89)\end{aligned}$$

The first three terms on the right-hand side of equation (89) can be further simplified with the Taylor expansion as follows:

$$F(x_2 - \tilde{c}\,\Delta x_1) = F - \tilde{c}\,\Delta x_1\frac{\partial F}{\partial x_2} + \frac{\tilde{c}^2\,\Delta x_1^2}{2}\frac{\partial^2 F}{\partial x_2^2} + O\left(\Delta x_1^3\right)$$

Equation (89) can be alternatively cast in the form

$$\begin{aligned}\langle \Psi, F(x_1+\Delta x_1, x_2)\rangle = &\langle \Psi, F(x_1, x_2 - \tilde{c}\,\Delta x_1)\rangle \\ &- \frac{\Delta x_1^2}{2}\left\langle \Psi, \tilde{c}\frac{\partial}{\partial x_2}(P_{\mathrm{CE}}F)\right\rangle \\ &+ O\left(\Delta x_1^3\right) \qquad (90)\end{aligned}$$

The inner product of Ψ with $F(x_1+\Delta x_1, x_2)$ gives the field variables ρu_1, $p + \rho u_1^2$, $\rho u_1 u_2$, and $\rho e u_1 + p u_1$ at $x_1 + \Delta x_1$ and x_2, and hence equation (90) constitutes the second-order accurate space-marching KNM for the Euler equations. It is interesting to note that the right-hand side of equation (90) contains an upwind term and an antidiffusive term. The antidiffusive term is absent in the first-order accurate KNM (eq. (81)). However, for second-order accuracy it is not enough to consider $F(x_1, x_2 - \tilde{c}\,\Delta x_1)$. The antidiffusive term can be merged with the upwind term by a slight manipulation to obtain a purely upwind space-marching KNM. First, we rewrite equation (89) as

$$\begin{aligned}\langle \Psi, F(x_1+\Delta x_1, x_2)\rangle = &\langle \Psi, F\rangle \\ &- \left\langle \Psi, \tilde{c}\,\Delta x_1\frac{\partial}{\partial x_2}\left(F + \frac{\Delta x_1}{2}P_{\mathrm{CE}}F\right)\right\rangle \\ &+ \frac{\Delta x_1^2}{2}\left\langle \Psi, \tilde{c}^2\frac{\partial^2 F}{\partial x_2^2}\right\rangle + O\left(\Delta x_1^3\right) \qquad (91)\end{aligned}$$

With the obvious relations

$$\begin{aligned}\langle \Psi, F\rangle &= \left\langle \Psi, F\left(1 + \frac{\Delta x_1}{2}P_{\mathrm{CE}}\right)\right\rangle \\ \left\langle \Psi, \tilde{c}^2\frac{\partial^2 F}{\partial x_2^2}\right\rangle &= \left\langle \Psi, \tilde{c}^2\frac{\partial^2}{\partial x_2^2}F\left(1 + \frac{\Delta x_1}{2}P_{\mathrm{CE}}\right)\right\rangle \\ &\quad + O\left(\Delta x_1^3\right)\end{aligned}$$

and the definition

$$f_{\mathrm{CE}} = F\left(1 + \frac{\Delta x_1}{2}P_{\mathrm{CE}}\right) \qquad (92)$$

equation (91) takes on the simple form

$$\langle \Psi, F(x_1+\Delta x_1, x_2)\rangle = \langle \Psi, f_{\mathrm{CE}}(x_1, x_2 - \tilde{c}\Delta x_1)\rangle + O\left(\Delta x_1^3\right) \qquad (93)$$

The velocity distribution f_{CE} is the Chapman-Enskog distribution function, and because of the positive sign in front of the second term in the brackets it is antidiffusive. Thus, the antidiffusion term in equation (90) appears in the form of a perturbation term in equation (92). The space-marching scheme in equation (93) now takes on a purely upwind form.

more familiar form

$$(\rho u_1)_j^{n+1} = \iiint v_1 f_{CE}\left(x_{1_n}, x_{2_j} - \tilde{c}\,\Delta x_1\right) dv_1\, dv_2\, dI \tag{94}$$

$$\left(p + \rho u_1^2\right)_j^{n+1} = \iiint v_1^2 f_{CE}\left(x_{1_n}, x_{2_j} - \tilde{c}\,\Delta x_1\right) dv_1\, dv_2\, dI \tag{95}$$

$$(\rho u_1 u_2)_j^{n+1} = \iiint v_1 v_2 f_{CE}\left(x_{1_n}, x_{2_j} - \tilde{c}\,\Delta x_1\right) dv_1\, dv_2\, dI \tag{96}$$

$$\begin{aligned}(\rho e u_1 + p u_1)_j^{n+1} &= \left(\frac{\gamma}{\gamma - 1} p u_1 + \frac{\rho u^2 u_1}{2}\right)_j^{n+1} \\ &= \iiint v_1 \left(I + \frac{v^2}{2}\right) \\ &\quad \times f_{CE}\left(x_{1_n}, x_{2_j} - \tilde{c}\,\Delta x_1\right) dv_1\, dv_2\, dI\end{aligned} \tag{97}$$

The only difference between the first- and second-order accurate schemes is that the first-order scheme uses the Maxwellian distribution and the second-order scheme uses the Chapman-Enskog distribution.

The integration with respect to I in equations (94) to (97) can be performed in closed form. Equations (94) to (97) then become

$$(\rho u_1)_j^{n+1} = \int_{-\infty}^{\infty}\int_{-\infty}^{\infty} v_1 \bar{f}_{CE}\left(x_{1_n}, x_{2_j} - \tilde{c}\,\Delta x_1\right) dv_1\, dv_2 \tag{98}$$

$$\left(p + \rho u_1^2\right)_j^{n+1} = \int_{-\infty}^{\infty}\int_{-\infty}^{\infty} v_1^2 \bar{f}_{CE}\left(x_{1_n}, x_{2_j} - \tilde{c}\Delta x_1\right) dv_1 dv_2 \tag{99}$$

$$(\rho u_1 u_2)_j^{n+1} = \int_{-\infty}^{\infty}\int_{-\infty}^{\infty} v_1 v_2 \bar{f}_{CE}\left(x_{1_n} x_{2_j} - \tilde{c}\,\Delta x_1\right) dv_1\, dv_2 \tag{100}$$

$$\begin{aligned}(\rho e u_1 + p u_1)_j^{n+1} &= \int_{-\infty}^{\infty}\int_{-\infty}^{\infty} \\ &\quad \times v_1 \bar{\bar{f}}_{CE}\left(x_{1_n}, x_{2_j} - \tilde{c}\,\Delta x_1\right) \\ &\quad \times I_o\left(x_{2_j} - \tilde{c}\,\Delta x_1\right) dv_1\, dv_2 \\ &\quad + \int_{-\infty}^{\infty}\int_{-\infty}^{\infty} \frac{v_1 v^2}{2} \\ &\quad \times \bar{f}_{CE}\left(x_{1_n}, x_{2_j} - \tilde{c}\,\Delta x_1\right) dv_1\, dv_2\end{aligned} \tag{101}$$

where

$$\bar{f}_{CE} = \tilde{F}\left(1 + \frac{\Delta x_1}{2}\bar{P}_{CE}\right)$$

$$\bar{\bar{f}}_{CE} = \tilde{F}\left(1 + \frac{\Delta x_1}{2}\bar{\bar{P}}_{CE}\right)$$

$\tilde{F}$ = Contracted local Maxwellian distribution

$$= \frac{\rho}{2\pi RT} \exp\left[-\frac{(v_1 - u_1)^2 + (v_2 - u_2)^2}{2RT}\right]$$

$$\begin{aligned}\bar{P}_{CE} &= \frac{1}{\rho}\left(\frac{\partial \rho}{\partial x_1} + \tilde{c}\frac{\partial \rho}{\partial x_2}\right)\left[2 - \frac{(v_1 - u_1)^2 + (v_2 - u_2)^2}{2RT}\right] \\ &\quad + \left(\frac{\partial u_1}{\partial x_1} + \tilde{c}\frac{\partial u_1}{\partial x_2}\right)\frac{v_1 - u_1}{RT} + \left(\frac{\partial u_2}{\partial x_1} + \tilde{c}\frac{\partial u_2}{\partial x_2}\right)\frac{v_2 - u_2}{RT} \\ &\quad + \frac{1}{p}\left(\frac{\partial p}{\partial x_1} + \tilde{c}\frac{\partial p}{\partial x_2}\right)\left[\frac{(v_1 - u_1)^2 + (v_2 - u_2)^2}{2RT} - 1\right]\end{aligned} \tag{102}$$

$$\begin{aligned}\bar{\bar{P}}_{CE} &= \frac{1}{\rho}\left(\frac{\partial \rho}{\partial x_1} + \tilde{c}\frac{\partial \rho}{\partial x_2}\right)\left[1 - \frac{(v_1 - u_1)^2 + (v_2 - u_2)^2}{2RT}\right] \\ &\quad + \left(\frac{\partial u_1}{\partial x_1} + \tilde{c}\frac{\partial u_1}{\partial x_2}\right)\frac{v_1 - u_1}{RT} + \left(\frac{\partial u_2}{\partial x_1} + \tilde{c}\frac{\partial u_2}{\partial x_2}\right)\frac{v_2 - u_2}{RT} \\ &\quad + \frac{1}{p}\left(\frac{\partial p}{\partial x_1} + \tilde{c}\frac{\partial p}{\partial x_2}\right)\frac{(v_1 - u_1)^2 + (v_2 - u_2)^2}{2RT}\end{aligned} \tag{103}$$

The partial derivatives of ρ, u_1, u_2, and p with respect to x_1 in equations (102) and (103) are replaced in terms of their x_2 derivatives by using the equations of appendix D. The x_2 derivative can be evaluated at mesh points by using, for example, central differencing. The numerical solution obtained with the KNM scheme will then be second-order accurate both in x_1 and x_2, provided the integration with respect to v_1 and v_2 is done sufficiently accurately.

Computed Results

In this section, we consider the application of the kinetic numerical method (KNM) to two test cases. The time-marching KNM developed previously for the unsteady Euler equations is applied to the one-dimensional shock-tube problem. The space-marching KNM is then applied to the shock-reflection problem.

Application of KNM to Shock-Tube Problem

For the application of the KNM to a one-dimensional shock-tube problem, we assume that the pressure p, temperature T, density ρ, and velocity u at time $t = 0$ sec are given by

$$\frac{\rho_{HP}}{\rho_{LP}} = \frac{p_{HP}}{p_{LP}} = 5.0$$

$$\frac{T_{HP}}{T_{LP}} = 1.0$$

$$u_{HP} = u_{LP} = 0$$

where HP and LP denote, respectively, the values corresponding to the high-pressure and low-pressure sides of the shock tube. The initial value of temperature is assumed to be 300 K and the gas constant per unit mass is $R = 287$ J/K. Results of computations are shown in figures 1 to 6. Distributions and interpolation schemes assumed in the computations are summarized in the following table.

Fig.	Distribution	Interpolation scheme	Courant number	J	t_A, sec
1, 2	Maxwellian	Linear	0.95	101	0.00083
3, 4	Chapman-Enskog	Eq. (63)	.95	101	.00041
5, 6	Chapman-Enskog	Eqs. (63) and (65)	.95	101	.00041

In this table J is the number of mesh points used and t_A is the time up to which the solution is advanced. The Neumann boundary condition has been used for all computations. In the KNM formulation, boundary conditions are required to determine the values of $\tilde{F}\left(t_n, x_j - v\,\Delta t, v\right)$ whenever $x_j - v\,\Delta t$ is outside the computational domain $x_{1,L} \leq x \leq x_{1,U}$. For the Neumann boundary condition at $x_1 = x_{1,L}$ and $x_1 = x_{1,U}$, the values of $\tilde{F}\left(x_j - v\,\Delta t\right)$ outside the computational domain are given by

$$\tilde{F}\left(x_j - v\,\Delta t\right) = \begin{cases} \tilde{F}\left(x_{1,L}, v, I\right) & \left(x_j - v\,\Delta t \leq x_{1,L}\right) \\ \tilde{F}\left(x_{1,U}, v, I\right) & \left(x_j - v\,\Delta t \geq x_{1,U}\right) \end{cases}$$

Plots of field variables against x presented in figures 1 and 2 show no pre- and post-shock oscillations. This is expected because of the TVNI property of the first-order accurate KNM. However, the shock and contact surfaces are badly smeared. This smearing confirms that the first-order KNM contains a large amount of numerical viscosity. The results of computations with the Chapman-Enskog distribution are shown in figures 3 and 4. The shock is much sharper, and this confirms the analysis of the preceding section. It is shown that the Chapman-Enskog distribution reduces the numerical viscosity in the KNM considerably and the numerical viscosity goes like $O(\Delta t^2)$. The sharpness of the shock, therefore, depends on Δt. The velocity and temperature, however, show marked fluctuations in the neighborhood of the shock as well as in the proximity of the contact surface. Use of the interpolation scheme (eqs. (63) and (65)) makes the KNM satisfy the TVNI property. This modified second-order accurate KNM is expected to do much better, and the results shown in figures 5 and 6 do indeed confirm this. The oscillations near the shock and the contact surface are considerably suppressed. However, the density plots of figures 3 and 5 reveal that the shock has been smeared somewhat as a consequence of the TVNI modification compared with the case when the interpolation is done with equation (63).

As mentioned before, the Chapman-Enskog distribution is not uniformly valid in v-space and in fact becomes negative for $v > O\left(\Delta t^{-1/3}\right)$. Thus, the distribution assumed in the computations is not right for fast molecules which penetrate through the discontinuity. It is here that work of Narasimha (ref. 11) on uniformly asymptotic expansion for f may help a great deal. In particular, the precursor distribution moving downstream in the neighborhood of the shock is likely to improve the KNM even more.

Application of KNM to Shock-Reflection Problem

The second-order accurate space-marching KNM developed previously is applied to the case of an oblique shock reflecting from a flat plate. Figure 7 shows a Cartesian grid system with 61 points along the X_1-axis and 21 points along the X_2-axis. The flat plate is on the X_1-axis and the computational domain is

$$x_{1,L} \leq x_1 \leq x_{1,U}$$
$$x_{2,L} \leq x_2 \leq x_{2,U}$$

An oblique shock with Mach number $M_1 = 2.9$ and deflection angle $\delta = 11°$ enters the computational domain at the point $\left(x_{1,L}, x_{2,U}\right)$. The shock, after undergoing reflection at the bottom flat plate, exits through the right-hand boundary of the domain. The initial conditions for the left-hand boundary are obtained from the uniform flow parallel to the X_1-axis at all mesh points except $\left(x_{1,L}, x_{2,U}\right)$. At this point the flow corresponds to conditions downstream of the oblique shock.

To advance the solution from line n to $n+1$, a scheme for numerical quadrature and a boundary strategy are required. The quadrature in equations (98) to (101) is performed with the product rule

$$\int_A^B \int_{A'}^{B'} h\left(x_1, x_2\right) dx_1\, dx_2 = \sum_i \sum_j w_i w_j h\left(x_{1_i}, x_{2_j}\right)$$

where w_i and w_j are the weights for the one-dimensional Simpson quadrature scheme. While performing the numerical quadrature, we need to evaluate the Chapman-Enskog distribution function f_{CE} at various mesh points. For some values of $\tilde{c}$, the point $x_{2_j} - \tilde{c}\,\Delta x_1$ may be out of the domain. Consequently, boundary conditions are then required to

calculate $f_{\mathrm{CE}}\left(x_{1_n}, x_{2_j} - c\,\Delta x_1\right)$. Two possibilities arise: $x_2 - c\,\Delta t \leq X_{2,L}$ or $x_2 - c\,\Delta t \geq X_{2,U}$.

For the shock-reflection problem, the flow tangency condition has to be imposed at the lower boundary (which is a solid wall), and the Neumann condition can be used at the upper boundary (which is fictitious). The details are as follows. Let x_2' be the position from which fluid particles arrive at x_2 during the time-like interval Δx_1. Obviously, $x_2' = x_2 - \tilde{c}\,\Delta x_1$ if $x_{2,L} \leq x_2 - \tilde{c}\,\Delta x_1 \leq x_{2,U}$. If, however, $x_2 - \tilde{c}\,\Delta x_1 \geq x_{2,U}$, then set $x_2' = x_{2,U}$. This ensures that the Neumann boundary condition is imposed on the upper boundary.

For positive values of $\tilde{c}$, the point $x_2 - \tilde{c}\,\Delta x_1$ can be below the lower wall, that is, $x_2 - \tilde{c}\,\Delta x_1$ can be less than $x_{2,L}$. In such a case, a specular reflection model is used to satisfy the flow tangency condition. The value of x_2' can be obtained with

$$x_2' = x_{2,L} + \tilde{c}\,(\Delta x_1 - \Delta \bar{x}_1)$$

$$\Delta \bar{x}_1 = \frac{x_2 - x_{2,L}}{\tilde{c}}$$

The particle velocity after the reflection at the wall is $-\tilde{c}$. Physically speaking, the gas-surface model consists of the fluid particle starting at x_2', traveling for $\Delta x_1 - \Delta \bar{x}_1$ at $-\tilde{c}$, and then traveling up to x_2 for the interval $\Delta \bar{x}_1$ with reversed velocity. For each pair of values x_2 and $\tilde{c}$, we determine x_2' and $\tilde{c}'$ and then use these values in calculating $f_{\mathrm{CE}}\left(x_{1_n}, x_2', v_1, \tilde{c}'\right)$ to be further used in the numerical integration.

The numerical integration in equations (98) to (101) generates the conservative variables

$$U_1 = \rho u_1$$

$$U_2 = p + \rho u_1^2$$

$$U_3 = \rho u_1 u_2$$

$$U_4 = (\rho e + p)u_1 = \left(\frac{\gamma}{\gamma - 1}p + \frac{\rho u^2}{2}\right) u_1$$

The field variables ρ, u_1, u_2, and p are given by

$$u_1 = \frac{\frac{\gamma U_2}{\gamma - 1} + \left[\left(\frac{\gamma U_2}{\gamma - 1}\right)^2 - \frac{\gamma + 1}{\gamma - 1}\left(2U_1 U_4 - U_3^2\right)\right]^{1/2}}{\frac{\gamma + 1}{\gamma - 1} U_1}$$

$$\rho = \frac{U_1}{u_1}$$

$$u_2 = \frac{U_3}{U_1}$$

$$p = U_2 - u_1 U_1$$

Finally, to evaluate $f_{\mathrm{CE}}\left(x_{1_n}, x_{2_j} - \tilde{c}\,\Delta x_1\right)$ whenever $x_{2_j} - \tilde{c}\,\Delta x_1$ is not coincident with a mesh point, an interpolation scheme is essential. The flux limiting method described previously can be used to make the KNM a TVD method.

The results of the computation are shown in figures 8 to 12. The pressure contours obtained with the flux limiting interpolation are depicted in figure 8. Figures 9 to 12 show the pressure plots at two stations. Also shown on these plots are the results with second- and third-order TVD methods of Chakravarthy and Osher (ref. 12). The position of the reflected shock given by the KNM agrees better with the position given by the third-order TVD method than with that given by the second-order TVD method.

Review and Discussion

A new upwind method, called the kinetic numerical method (KNM), for obtaining the numerical solution of the Euler equations has been presented. The method exploits the well-known fact that the moments of the Boltzmann equation of the kinetic theory of gases are the Euler equations when the distribution function is Maxwellian. Thus, every method for the solution of the Boltzmann equation can be mapped to a method for the solution of the Euler equations provided the distribution function is Maxwellian. The mapped-method strategy has been used to develop the KNM, which is explicit, is upwinding, satisfies the entropy condition, and is highly vectorizable. Further, it can be made total variation diminishing (TVD) by using a suitable interpolation strategy for evaluating the Maxwellian distribution. A unique aspect of the present work is the use of the antidiffusive Chapman-Enskog distribution in developing a second-order accurate KNM. An immediate consequence of the use of the Chapman-Enskog distribution is that by modifying slightly the expressions for $\boldsymbol{\tau}$ and $\mathbf{q}$ to include physical viscous stress and heat flux, the KNM can be applied to obtain the solution of the Navier-Stokes equations.

An important difference between the KNM and other methods is the treatment of the boundary conditions. On any surface (bounding the computational domain) where boundary conditions are imposed, the velocity distribution function f can be regarded as consisting of f^+ and f^- standing respectively for the particles moving towards and away from the surface. The particles corresponding to f^+ carry information out of the domain, whereas those corresponding to f^- cause an inflow of information from outside. It is then possible to treat the boundary conditions in a

physically meaningful way. For example, in the application of the KNM to the two-dimensional shock-reflection problem, particles reflect with reversed normal velocity after colliding with the solid wall. The distribution f^+ is then the velocity distribution due to incident particles, whereas f^- corresponds to the reflected particles. The flow tangency condition is then satisfied by simply requiring that

$$f^-(v_n, v_t) = f^+(-v_n, v_t) \qquad (v_n < 0)$$

Another unique feature of the KNM is that the solution at every field point x_2 is due to the particles directly arriving from any other point x_2'. The solution is also due to particles starting from x_2' undergoing interaction with the solid surface and then arriving at x_2 with different particle velocities. In terms of f^+ and f^-, we can state that the solution at x_2 is influenced by both f^+ and f^-. For field points close to the solid boundary, the solution will be strongly influenced by particles reflected from the boundary. These two kinds of contributions to the solution are physically meaningful and allow the KNM to treat the boundary conditions in a way that is not found in many other finite-difference schemes. In view of the above advantages of KNM, it is believed that the approach of developing mapped methods will lead to the construction of numerical schemes for the Euler and Navier-Stokes equations not known heretofore.

NASA Langley Research Center
Hampton, VA 23665-5225
July 10, 1986

Appendix A

The Connection Between the Boltzmann Equation and the Euler Equations

The Boltzmann equation for f is

$$\frac{\partial f}{\partial t} + \mathbf{v} \cdot \frac{\partial f}{\partial \mathbf{x}} = J(f, f) \tag{A1}$$

The collision term J has collisional invariants 1, $\mathbf{v}$, and $I + \frac{v^2}{2}$, that is,

$$\iint \psi(\mathbf{v}, I) J(f, f)\, D\mathbf{v}\, dI = 0 \tag{A2}$$

where $\psi = 1$, $\mathbf{v}$, and $I + \frac{v^2}{2}$ and $D\mathbf{v} = dv_1\, dv_2\, dv_3$. Equation (A2) is a direct consequence of the conservation of mass, momentum, and energy during a collision. Substituting equation (A1) into (A2) yields

$$\iint \psi(\mathbf{v}, I) \left(\frac{\partial f}{\partial t} + \mathbf{v} \cdot \frac{\partial f}{\partial \mathbf{x}} \right) D\mathbf{v}\, dI = 0 \tag{A3}$$

The field variables density $\rho = \rho(t, \mathbf{x})$, fluid velocity $\mathbf{u} = \mathbf{u}(t, \mathbf{x})$, and specific internal energy $e = e(t, \mathbf{x})$ are related to f through the following moment equations:

$$\left.\begin{aligned} \rho &= \iint f(t,\mathbf{x},\mathbf{v})\, D\mathbf{v}\, dI \\ \rho\mathbf{u} &= \iint \mathbf{v} f(t,\mathbf{x},\mathbf{v})\, D\mathbf{v}\, dI \\ \rho e &= \iint \left(I + \frac{v^2}{2} \right) f(t,\mathbf{x},\mathbf{v})\, D\mathbf{v}\, dI \end{aligned}\right\} \tag{A4}$$

The viscous stress tensor $\boldsymbol{\tau}$ and the heat flux vector $\mathbf{q}$ are defined by

$$p\delta_{ij} - \tau_{ij} = \iint c_i c_j f\, D\mathbf{v}\, dI \tag{A5}$$

$$q_i = -\iint \left(I + \frac{c^2}{2} \right) c_i f\, D\mathbf{v}\, dI \tag{A6}$$

where c_i is the peculiar velocity $v_i - u_i$, δ_{ij} is the Kronecker delta, and p is the static pressure. Using equations (A4), (A5), and (A6) we have

$$\int \begin{bmatrix} 1 \\ \mathbf{v} \\ I + \frac{v^2}{2} \end{bmatrix} \frac{\partial f}{\partial t} D\mathbf{v}\, dI = \frac{\partial}{\partial t} \begin{bmatrix} \rho \\ \rho\mathbf{u} \\ \rho e \end{bmatrix}$$

and

$$\iint \begin{bmatrix} 1 \\ v_i \\ I + \frac{v^2}{2} \end{bmatrix} v_j \frac{\partial f}{\partial x_j} D\mathbf{v}\, dI = \frac{\partial}{\partial x_j} \iint \begin{bmatrix} v_j \\ v_i v_j \\ \left(I + \frac{v^2}{2} \right) v_j \end{bmatrix} f\, D\mathbf{v}\, dI$$

Now,

$$\iint v_i v_j f \, D\mathbf{v} \, dI = \iint \left(c_i c_j + c_i u_j + c_j u_i + u_i u_j \right) f \, D\mathbf{v} \, dI$$
$$= p\delta_{ij} - \tau_{ij} + \rho u_i u_j$$

and

$$\iint \left(I + \frac{v^2}{2} \right) v_j f \, D\mathbf{v} \, dI = \iint \left(I + \frac{v^2}{2} \right) u_j f \, D\mathbf{v} \, dI$$
$$+ \iint \left(I + \frac{v^2}{2} \right) c_j f \, D\mathbf{v} \, dI$$
$$= \rho e u_j + \iint \left[I + \frac{(\mathbf{v} - \mathbf{u})^2}{2} + \frac{u^2}{2} + c_i u_i \right] c_j \, D\mathbf{v} \, dI$$
$$= \rho e u_j - q_j + \left(p\delta_{ij} - \tau_{ij} \right) u_i$$

Equations (A4) therefore yield

$$\left.\begin{aligned} \frac{\partial \rho}{\partial t} + \frac{\partial}{\partial x_j} \left(\rho u_j \right) &= 0 \\ \frac{\partial}{\partial t} \left(\rho u_i \right) + \frac{\partial}{\partial x_j} \left(\rho u_i u_j + p\delta_{ij} \right) &= \frac{\partial \tau_{ij}}{\partial_{xj}} \\ \frac{\partial}{\partial t} (\rho e) + \frac{\partial}{\partial x_j} \left(\rho e u_j + p u_j \right) &= \frac{\partial}{\partial x_j} \left(q_j + u_i \tau_{ij} \right) \end{aligned}\right\} \tag{A7}$$

The above moment equations reduce to the Euler equations if

$$\tau_{ij} = 0 \qquad \text{and} \qquad q_j = 0$$

In general, for an arbitrary f, the moments τ_{ij} and q_j are not zero. However, if f is the Maxwellian distribution defined by

$$f = F = \frac{\rho}{(2\pi RT)^{3/2}} \exp \left[-\frac{(\mathbf{v} - \mathbf{u})^2}{2RT} \right] \frac{\exp(-I/I_o)}{I_o} \tag{A8}$$

then τ_{ij} and q_j vanish. Here R is the gas constant per unit mass, T is the temperature, and I_o is the internal energy due to nontranslational degrees of freedom. The value I_o is related to T through the relation

$$I_o = \frac{\left(2 + D_f \right) - \gamma D_f}{2(\gamma - 1)} RT$$

where D_f is the number of translational degrees of freedom and γ is the ratio of the specific heats. When f is a Maxwellian distribution,

$$\iint c_1 c_2 f \, D\mathbf{v} \, dI = \iint c_2 c_3 f \, D\mathbf{v} \, dI = \iint c_3 c_1 f \, D\mathbf{v} \, dI = 0$$
$$\iint c_1^2 f \, D\mathbf{v} \, dI = \iint c_2^2 f \, D\mathbf{v} \, dI = \iint c_3^2 f \, D\mathbf{v} \, dI = \rho RT$$

The normal stress tensor components τ_{11}, τ_{22}, and τ_{33} can be absorbed in the definition of p, and equation (A5) then yields

$$p = \iint c_1^2 F \, D\mathbf{v} \, dI = \rho RT \tag{A9}$$

Appendix B

Elimination of Time Derivatives

The one-dimensional Euler equations are

$$\frac{\partial}{\partial t}(\rho) + \frac{\partial}{\partial x}(\rho u) = 0 \tag{B1}$$

$$\frac{\partial}{\partial t}(\rho u) + \frac{\partial}{\partial x}(p + \rho u^2) = 0 \tag{B2}$$

$$\frac{\partial}{\partial t}(\rho e) + \frac{\partial}{\partial x}(\rho u e + p u) = 0 \tag{B3}$$

where

$$e = \frac{RT}{\gamma - 1} + \frac{u^2}{2} = \frac{p}{\rho(\gamma - 1)} + \frac{u^2}{2} \tag{B4}$$

The pressure p is related to e through

$$p = \rho(\gamma - 1)\left(e - \frac{u^2}{2}\right) \tag{B5}$$

The objective is to replace

$$\frac{\partial}{\partial t}(\rho), \quad \frac{\partial}{\partial t}(\rho u), \quad \frac{\partial}{\partial t}(\rho e), \quad \frac{\partial^2}{\partial t^2}(\rho), \quad \frac{\partial^2}{\partial t^2}(\rho u), \text{ and } \quad \frac{\partial^2}{\partial t^2}(\rho e)$$

in terms of the space derivatives. Taking ρ first, we have

$$\left.\begin{aligned} \frac{\partial}{\partial t}(\rho) &= -\frac{\partial}{\partial x}(\rho u) \\ \frac{\partial^2}{\partial t^2}(\rho) &= -\frac{\partial}{\partial t}\frac{\partial}{\partial x}(\rho u) = -\frac{\partial}{\partial x}\frac{\partial}{\partial t}(\rho u) = \frac{\partial^2}{\partial x^2}(p + \rho u^2) \end{aligned}\right\} \tag{B6}$$

Taking ρu next, we have

$$\frac{\partial}{\partial t}(\rho u) = -\frac{\partial}{\partial x}(p + \rho u^2) \tag{B7}$$

$$\frac{\partial^2}{\partial t^2}(\rho u) = -\frac{\partial}{\partial x}\frac{\partial}{\partial t}(p + \rho u^2) \tag{B8}$$

Now, the energy equation can be written as

$$\frac{\partial}{\partial t}\left(p + \frac{\gamma - 1}{2}\rho u^2\right) + \frac{\partial}{\partial x}\left(\gamma p u + \frac{\gamma + 1}{2}\rho u^3\right) = 0 \tag{B9}$$

which is obtained by eliminating e in terms of p in equation (B3) through the use of equation (B4). Hence,

$$\begin{aligned} \frac{\partial}{\partial t}(p + \rho u^2) &= \frac{\partial}{\partial t}\left(p + \frac{\gamma - 1}{2}\rho u^2\right) + \frac{3 - \gamma}{2}\frac{\partial}{\partial t}(\rho u^2) \\ &= -\frac{\partial}{\partial x}\left(\gamma p u + \frac{\gamma - 1}{2}\rho u^3\right) + \frac{3 - \gamma}{2}\frac{\partial}{\partial t}(\rho u^2) \end{aligned} \tag{B10}$$

as a result of equation (B9). For the time derivative of ρu^2 we have

$$\begin{aligned}\frac{\partial}{\partial t}(\rho u^2) &= u^2\frac{\partial}{\partial t}(\rho) + 2\rho u\frac{\partial}{\partial t}(u) \\ &= 2u\frac{\partial}{\partial t}(\rho u) - u^2\frac{\partial}{\partial t}(\rho) \\ &= -2u\frac{\partial}{\partial x}(p + \rho u^2) + u^2\frac{\partial}{\partial x}(\rho u)\end{aligned}$$

where equations (B1) and (B2) have been used. Equation (B10) then yields

$$\begin{aligned}\frac{\partial}{\partial t}(p + \rho u^2) = &-\frac{\partial}{\partial x}\left(\gamma p u + \frac{\gamma - 1}{2}\rho u^3\right) + \frac{3-\gamma}{2}u^2\frac{\partial}{\partial x}(\rho u) \\ &-(3-\gamma)u\frac{\partial}{\partial x}(p + \rho u^2)\end{aligned}$$

Slight manipulation gives

$$\begin{aligned}\frac{\partial}{\partial t}(p + pu^2) = &-\frac{\partial}{\partial x}\left[\gamma p u + \frac{\gamma - 1}{2}\rho u^3 + (3-\gamma)pu + (3-\gamma)\rho u^3\right. \\ &\left. - \frac{3-\gamma}{2}\rho u^3\right] + (3-\gamma)\left(p + \rho u^2 - \rho u^2\right)\frac{\partial}{\partial x}(u) \\ = &-\frac{\partial}{\partial x}(3pu + \rho u^3) + (3-\gamma)p\frac{\partial}{\partial x}(u) \qquad \text{(B11)}\end{aligned}$$

Note that

$$\begin{aligned}\iint v^3 F\, dv\, dI &= \iint \left\{(v-u)^3 + 3(v-u)^2 u + 3(v-u)u^2 + u^3\right\} F\, dv\, dI \\ &= 3pu + \rho u^3\end{aligned}$$

Equation (B11) can then be written as

$$\frac{\partial}{\partial t}(p + \rho u^2) = -\frac{\partial}{\partial x}\iint v^3 F\, dv\, dI + (3-\gamma)p\frac{\partial}{\partial x}(u) \qquad \text{(B12)}$$

Combining equations (B12) and (B8) gives

$$\begin{aligned}\frac{\partial^2}{\partial t^2}(\rho u) &= \frac{\partial^2}{\partial x^2}(3pu + \rho u^3) - \frac{\partial}{\partial x}\left[(3-\gamma)p\frac{\partial}{\partial x}(u)\right] \\ &= \frac{\partial^2}{\partial x^2}\int v^3 F\, dv\, dI - \frac{\partial}{\partial x}\left[(3-\gamma)p\frac{\partial}{\partial x}(u)\right] \qquad \text{(B13)}\end{aligned}$$

Finally, let us consider ρe. Its second-order time derivative is given by

$$\frac{\partial^2}{\partial t^2}(\rho e) = -\frac{\partial}{\partial x}\frac{\partial}{\partial t}(\rho u e + pu) \qquad \text{(B14)}$$

For the time derivative of $\rho u e + pu$ we have

$$\frac{\partial}{\partial t}(\rho e u + pu) = \frac{\partial}{\partial t}\left\{u\left[\rho e + \rho(\gamma - 1)\left(e - \frac{u^2}{2}\right)\right]\right\}$$

where p has been eliminated in terms of e with equation (B5). After slight simplification we obtain

$$\begin{aligned}\frac{\partial}{\partial t}(\rho eu + pu) &= \frac{\partial}{\partial t}(\rho eu\gamma) - \frac{\gamma-1}{2}\frac{\partial}{\partial t}(\rho u^3) \\ &= \gamma\frac{\partial}{\partial t}\left(\rho e\frac{\rho u}{\rho}\right) - \frac{\gamma-1}{2}\frac{\partial}{\partial t}\frac{\rho^3u^3}{\rho^2} \\ &= \gamma\left[u\frac{\partial}{\partial t}(\rho e) + e\frac{\partial}{\partial t}(\rho u) - eu\frac{\partial}{\partial t}(\rho)\right] \\ &\quad - \frac{3(\gamma-1)}{2}u^2\frac{\partial}{\partial t}(\rho u) + (\gamma-1)u^3\frac{\partial}{\partial t}(\rho)\end{aligned}$$

which is a relation containing first-order time derivatives of ρ, ρu, and ρe. Grouping terms together we have

$$\begin{aligned}\frac{\partial}{\partial t}(\rho eu + pu) = \gamma u\frac{\partial}{\partial t}(\rho e) &+ \left[\gamma e - \frac{3(\gamma-1)}{2}u^2\right]\frac{\partial}{\partial t}(\rho u) \\ &+ \left[(\gamma-1)u^3 - \gamma ue\right]\frac{\partial}{\partial t}(\rho)\end{aligned}$$

Using equations (B1), (B2), and (B3) to eliminate time derivatives, we obtain

$$\begin{aligned}\frac{\partial}{\partial t}(\rho eu + pu) = -\gamma u\frac{\partial}{\partial x}(\rho eu + pu) &- \left[\gamma e - \frac{3(\gamma-1)}{2}u^2\right]\frac{\partial}{\partial x}(p + \rho u^2) \\ &- \left[(\gamma-1)u^3 - \gamma ue\right]\frac{\partial}{\partial x}(\rho u)\end{aligned} \tag{B15}$$

Substitution for e in terms of p through the use of equation (B4) yields

$$\begin{aligned}\frac{\partial}{\partial t}(\rho eu + pu) = -\gamma u\frac{\partial}{\partial x}&\left(\frac{\gamma}{\gamma-1}pu + \frac{\rho u^3}{2}\right) - \left(\frac{\gamma}{\gamma-1}\frac{p}{\rho} + \frac{3-2\gamma}{2}u^2\right) \\ &\times\frac{\partial}{\partial x}(p + \rho u^2) - \left[\frac{\gamma-2}{2}u^3 - \frac{\gamma pu}{(\gamma-1)\rho}\right]\frac{\partial}{\partial x}(\rho u)\end{aligned} \tag{B16}$$

We can replace each term on the right-hand side of equation (B16) using the identity

$$\mathrm{A}\frac{\partial}{\partial x}(\mathrm{B}) = \frac{\partial}{\partial x}(\mathrm{AB}) - \mathrm{B}\frac{\partial}{\partial x}(\mathrm{A})$$

Equation (B16) then reduces to

$$\begin{aligned}\frac{\partial}{\partial t}(\rho eu + pu) = -\frac{\partial}{\partial x}&\left(\frac{\gamma^2}{\gamma-1}pu^2 + \frac{\gamma}{2}\rho u^4 + \frac{\gamma}{\gamma-1}\frac{p^2}{\rho} + \frac{\gamma}{\gamma-1}pu^2 + \frac{3-2\gamma}{2}pu^2\right. \\ &\left. + \frac{3-2\gamma}{2}\rho u^4 + \frac{\gamma-2}{2}\rho u^4 - \frac{\gamma}{\gamma-1}pu^2\right) \\ &+ \left(\frac{\gamma^2}{\gamma-1}pu + \frac{\gamma}{2}\rho u^3\right)\frac{\partial u}{\partial x} + (p + \rho u^2)\frac{\partial}{\partial x}\left(\frac{\gamma}{\gamma-1}\frac{p}{\rho}\right. \\ &\left. + \frac{3-2\gamma}{2}u^2\right) + \rho u\frac{\partial}{\partial x}\left(\frac{\gamma-2}{2}u^3 - \frac{\gamma pu}{\rho(\gamma-1)}\right) \\ = \frac{\partial}{\partial x}&\left[\frac{5\gamma-3}{2(\gamma-1)}pu^2 + \frac{\gamma}{\gamma-1}\frac{p^2}{\rho} + \frac{1}{2}\rho u^4\right] + \left(\frac{\gamma^2}{\gamma-1}pu + \frac{\gamma}{2}\rho u^3\right)\frac{\partial u}{\partial x} \\ &+ (p + \rho u^2)\frac{\partial}{\partial x}\left(\frac{\gamma}{\gamma-1}\frac{p}{\rho} + \frac{3-2\gamma}{2}u^2\right) + \rho u\frac{\partial}{\partial x}\left[\frac{\gamma-2}{2}u^3 - \frac{\gamma pu}{\rho(\gamma-1)}\right]\end{aligned}$$

Finally, grouping terms containing $\frac{\partial}{\partial x}u$ and $\frac{\partial}{\partial x}\left(\frac{p}{\rho}\right)$, we obtain

$$\begin{aligned}\frac{\partial}{\partial t}(\rho eu+pu) &= -\frac{\partial}{\partial x}\left[\frac{5\gamma-3}{2(\gamma-1)}pu^2+\frac{\gamma}{\gamma-1}\frac{p^2}{\rho}+\frac{1}{2}\rho u^4\right]+\frac{\partial}{\partial x}(u)\\ &\quad\times\left[\frac{\gamma^2}{\gamma-1}pu+\frac{\gamma}{2}\rho u^3+(p+\rho u^2)(3-2\gamma)u+\frac{3}{2}(\gamma-1)\rho u^3\right.\\ &\quad\left.-\frac{p\gamma}{\gamma-1}u\right]+\left[(p+\rho u^2)\frac{\gamma}{\gamma-1}-\rho u^2\frac{\gamma}{\gamma-1}\right]\frac{\partial}{\partial x}\left(\frac{p}{\rho}\right)\\ &= -\frac{\partial}{\partial x}\left[\frac{5\gamma-3}{2(\gamma-1)}pu^2+\frac{\gamma}{\gamma-1}\frac{p^2}{\rho}+\frac{1}{2}\rho u^4\right]+(3-\gamma)pu\frac{\partial}{\partial x}(u)\\ &\quad+\frac{\gamma p}{\gamma-1}\frac{\partial}{\partial x}\left(\frac{p}{\rho}\right)\end{aligned}\tag{B17}$$

Note that

$$\begin{aligned}\iint\left(I+\frac{v^2}{2}\right)v^2F\,dv\,dI &= \iint Iv^2F\,dv\,dI+\frac{1}{2}\iint v^4F\,dv\,dI\\ &= I_o(p+\rho u^2)+\frac{1}{2}\iint\left[(v-u)^4+4(v-u)^3u+6(v-u)^2u^2\right.\\ &\quad\left.+4(v-u)u^3+u^4\right]F\,dv\,dI\\ &= \frac{3-\gamma}{2(\gamma-1)}\frac{p}{\rho}\left(p+\rho u^2\right)+\frac{1}{2}\left(\frac{3p^2}{\rho}+6pu^2+\rho u^4\right)\\ &= \frac{5\gamma-3}{2(\gamma-1)}pu^2+\frac{\gamma}{\gamma-1}\frac{p^2}{\rho}+\frac{1}{2}\rho u^4\end{aligned}\tag{B18}$$

Hence, equation (B17) can be written as

$$\begin{aligned}\frac{\partial}{\partial t}(\rho eu+pu) &= -\frac{\partial}{\partial x}\left[\iint\left(I+\frac{v^2}{2}\right)v^2F\,dv\,dI\right]+(3-\gamma)pu\frac{\partial}{\partial x}u\\ &\quad+\frac{\gamma p}{\gamma-1}\frac{\partial}{\partial x}\left(\frac{p}{\rho}\right)\end{aligned}$$

The second derivative of ρ with respect to t is thus given by

$$\begin{aligned}\frac{\partial^2}{\partial t^2}(\rho e) &= \frac{\partial^2}{\partial x^2}\left[\iint\left(I+\frac{v^2}{2}\right)v^2F\,dv\,dI\right]-\frac{\partial}{\partial x}\left[(3-\gamma)pu\frac{\partial u}{\partial x}\right]\\ &\quad-\frac{\partial}{\partial x}\left[\frac{\gamma}{\gamma-1}p\frac{\partial}{\partial x}\left(\frac{p}{\rho}\right)\right]\end{aligned}\tag{B19}$$

Appendix C

Chapman-Enskog Analysis

Consider the model Boltzmann equation

$$\frac{\partial f}{\partial t} + v\frac{\partial f}{\partial x} = \alpha(F - f) \tag{C1}$$

where

$$F = \frac{\rho}{I_o}\left(\frac{\beta}{\pi}\right)^{1/2} \exp\left[-\beta(v-u)^2 - I/I_o\right] \tag{C2}$$

$$\left.\begin{aligned} \beta &= \frac{1}{2RT} \\ I_o &= \frac{3-\gamma}{2(\gamma-1)}RT = \frac{3-\gamma}{4(\gamma-1)}\frac{1}{\beta} \end{aligned}\right\} \tag{C3}$$

and α is a time constant characteristic of collisions. Assume that $f = F\Phi$, where Φ is a function to be determined. Substitution in equation (C1) yields

$$\Phi = 1 - \frac{\Phi}{\alpha}\frac{1}{F}\left(\frac{\partial F}{\partial t} + v\frac{\partial F}{\partial x}\right) - \frac{F}{\alpha}\left(\frac{\partial \Phi}{\partial t} + v\frac{\partial \Phi}{\partial x}\right) \tag{C4}$$

Formal solution of equation (C4) can be written as

$$\Phi = \frac{1 - (F/\alpha)[(\partial\Phi/\partial t) + v(\partial\Phi/\partial x)]}{1 + (1/\alpha F)[(\partial F/\partial t) + v(\partial F/\partial x)]} \tag{C5}$$

If

$$\left|\frac{F}{\alpha}\left(\frac{\partial \Phi}{\partial t} + v\frac{\partial \Phi}{\partial x}\right)\right| << \left|\frac{\Phi}{\alpha}\frac{1}{F}\left(\frac{\partial F}{\partial t} + v\frac{\partial F}{\partial x}\right)\right|$$

then approximate solution for Φ is given by

$$\Phi \approx \frac{1}{1 + (1/\alpha F)[(\partial F/\partial t) + v(\partial F/\partial x)]}$$

Further, if $\left|\frac{1}{\alpha F}\left(\frac{\partial F}{\partial t} + v\frac{\partial F}{\partial x}\right)\right| << 1$, then $\Phi \approx 1 - \frac{1}{\alpha F}\left(\frac{\partial F}{\partial t} + v\frac{\partial F}{\partial x}\right)$

The Chapman-Enskog solution is

$$f_{\mathrm{CE}} = F\Phi = F\left[1 - \frac{1}{\alpha F}\left(\frac{\partial F}{\partial t} + \frac{\partial F}{\partial x}\right)\right] \tag{C6}$$

The next step in the Chapman-Enskog analysis consists of replacing $\frac{\partial F}{\partial t}$ with space derivatives determined with the Euler equations. For this purpose note that

$$\frac{1}{F}\left(\frac{\partial F}{\partial t} + v\frac{\partial F}{\partial x}\right) = \left(\frac{\partial}{\partial t} + v\frac{\partial}{\partial x}\right)\ln F$$

$$\ln F = \ln\rho + \frac{1}{2}\ln\beta - \frac{1}{2}\ln\pi - \beta(v-u)^2 - \ln I_o - \frac{I}{I_o}$$

Hence,

$$P_{CE} = \frac{1}{F}\left(\frac{\partial F}{\partial t} + v\frac{\partial F}{\partial x}\right)$$
$$= \frac{1}{\rho}\left(\frac{\partial \rho}{\partial t} + v\frac{\partial \rho}{\partial x}\right) + \left[\frac{1}{2\beta} - (v-u)^2\right]\left(\frac{\partial \beta}{\partial t} + v\frac{\partial \beta}{\partial x}\right)$$
$$+ 2\beta(v-u)\left(\frac{\partial u}{\partial t} + v\frac{\partial u}{\partial x}\right) + \left(\frac{I}{I_o^2} - \frac{I}{I_o}\right)\left(\frac{\partial I_o}{\partial t} + v\frac{\partial I_o}{\partial x}\right) \tag{C7}$$

From equation (C3) it follows that

$$\frac{1}{I_o}\left(\frac{\partial I_o}{\partial t} + v\frac{\partial I_o}{\partial x}\right) = -\frac{1}{\beta}\left(\frac{\partial \beta}{\partial t} + v\frac{\partial \beta}{\partial x}\right)$$

Equation (C7) therefore becomes

$$P_{CE} = \frac{1}{\rho}\left(\frac{\partial \rho}{\partial t} + v\frac{\partial \rho}{\partial x}\right) + 2\beta(v-u)\left(\frac{\partial u}{\partial t} + v\frac{\partial u}{\partial x}\right)$$
$$+ \left[\frac{3}{2\beta} - \frac{I}{B} - (v-u)^2\right]\left(\frac{\partial \beta}{\partial t} + v\frac{\partial \beta}{\partial x}\right) \tag{C8}$$

where

$$B = \frac{3-\gamma}{4(\gamma-1)}$$

Now, from the equation of continuity,

$$\frac{\partial \rho}{\partial t} = -u\frac{\partial \rho}{\partial x} - \rho\frac{\partial u}{\partial x}$$

From the momentum equation,

$$\frac{\partial u}{\partial t} = -\frac{1}{\rho}\frac{\partial p}{\partial x} - u\frac{\partial u}{\partial x}$$
$$= -\frac{1}{\rho}\frac{\partial}{\partial x}\left(\frac{\rho}{2\beta}\right) - u\frac{\partial u}{\partial x}$$
$$= -\frac{1}{2\rho\beta}\frac{\partial \rho}{\partial x} + \frac{1}{2\beta^2}\frac{\partial \beta}{\partial x} - u\frac{\partial u}{\partial x}$$

Thus,

$$\left.\begin{aligned}\frac{\partial \rho}{\partial t} + v\frac{\partial \rho}{\partial x} &= (v-u)\frac{\partial \rho}{\partial x} - \rho\frac{\partial u}{\partial x}\\ \frac{\partial u}{\partial t} + v\frac{\partial u}{\partial x} &= (v-u)\frac{\partial u}{\partial x} + \frac{1}{2\beta^2}\frac{\partial \beta}{\partial x} - \frac{1}{2\rho\beta}\frac{\partial \rho}{\partial x}\end{aligned}\right\} \tag{C9}$$

Substitution of equations (C9) into (C8) yields

$$P_{CE} = \left[2\beta(v-u)^2 - 1\right]\frac{\partial u}{\partial x} + \frac{v-u}{\beta}\frac{\partial \beta}{\partial x} + \left(\frac{\partial \beta}{\partial t} + v\frac{\partial \beta}{\partial x}\right)\left[\frac{3}{2\beta} - \frac{I}{B} - (v-u)^2\right] \tag{C10}$$

Now $\frac{\partial \beta}{\partial t}$ remains to be eliminated. The energy equation gives

$$\rho\frac{\partial e}{\partial t} + \rho u\frac{\partial e}{\partial x} + \frac{\partial}{\partial x}(pu) = 0$$

Substituting for p and e in terms of β by using equation (B4) and the equation of state, we obtain

$$\rho\left[-\frac{1}{2(\gamma-1)\beta^2}\frac{\partial\beta}{\partial t}+u\frac{\partial u}{\partial t}\right]+\rho u\left[-\frac{1}{2(\gamma-1)\beta^2}\frac{\partial\beta}{\partial x}+u\frac{\partial u}{\partial x}\right]$$
$$+\frac{\rho}{2\beta}\frac{\partial u}{\partial x}+u\frac{\partial p}{\partial x}=0$$

Using the momentum equation to remove $\frac{\partial u}{\partial t}$, we obtain

$$\frac{\partial\beta}{\partial t}=-u\frac{\partial\beta}{\partial x}+(\gamma-1)\beta\frac{\partial u}{\partial x}$$

or

$$\frac{\partial\beta}{\partial t}+v\frac{\partial\beta}{\partial x}=(v-u)\frac{\partial\beta}{\partial x}+(\gamma-1)\beta\frac{\partial u}{\partial x} \tag{C11}$$

Substituting $\frac{\partial\beta}{\partial t}+v\frac{\partial\beta}{\partial x}$ from equation (C11) into (C10) gives

$$\begin{aligned}P_{\mathrm{CE}}&=\left[2\beta(v-u)^2-1\right]\frac{\partial u}{\partial x}+\frac{v-u}{\beta}\frac{\partial\beta}{\partial x}+\left[\frac{3}{2\beta}-\frac{I}{B}-(v-u)^2\right]\\&\quad\times\left[(v-u)\frac{\partial\beta}{\partial x}+(\gamma-1)\beta\frac{\partial u}{\partial x}\right]\\&=\left[\frac{3\gamma-5}{2}+(3-\gamma)\beta(v-u)^2-\frac{(\gamma-1)\beta I}{B}\right]\frac{\partial u}{\partial x}\\&\quad+\left[\frac{5(v-u)}{2\beta}-\frac{I(v-u)}{B}-(v-u)^3\right]\frac{\partial\beta}{\partial x}\end{aligned} \tag{C12}$$

Substituting for B in equation (C12) gives the following result:

$$\begin{aligned}P_{\mathrm{CE}}&=\left[\frac{3\gamma-5}{2}+(3-\gamma)\beta(v-u)^2-\frac{4(\gamma-1)^2}{3-\gamma}\beta I\right]\frac{\partial u}{\partial x}\\&\quad+\left[\frac{5(v-u)}{2\beta}-\frac{4(\gamma-1)}{3-\gamma}I(v-u)-(v-u)^3\right]\frac{\partial\beta}{\partial x}\end{aligned} \tag{C13}$$

Note that P_{CE} is a polynomial in $v-u$ and I. The Chapman-Enskog distribution

$$f_{\mathrm{CE}}=F\left[1-\frac{P_{\mathrm{CE}}}{\alpha}\right] \tag{C14}$$

is thus a perturbation over the local Maxwellian distribution F. Some important properties of f_{CE} are worth noting. First, observe that

$$\iint F\,dv\,dI=\rho,\quad\iint vF\,dv\,dI=\rho u,\quad\iint v^2F\,dv\,dI=p+\rho u^2,$$

$$\iint(v-u)^2F\,dv\,dI=p,\quad\iint(v-u)F\,dv\,dI=0,\quad\iint IF\,dv\,dI=\rho I_o,$$

$$\iint I^2F\,dv\,dI=2\rho I_o^2,\quad\iint(v-u)^3F\,dv\,dI=0,\quad\iint(v-u)^4F\,dv\,dI=\frac{3p}{4\beta^2},$$

$$\iint(v-u)^6F\,dv\,dI=\frac{15\rho}{8\beta^3}$$

With these definite integrals the following results are obtained:

$$\iint \begin{bmatrix} 1 \\ v \\ I + \frac{v^2}{2} \end{bmatrix} (f_{CE} - F) dv\, dI = 0 \tag{C15}$$

$$\iint (v-u)^2 f_{CE}\, dv\, dI = p - \tau_{CE} \tag{C16}$$

$$\iint -\left[I + \frac{(v-u)^2}{2}\right](v-u) f_{CE}\, dv\, dI = q_{CE} = \frac{\gamma}{\gamma - 1}\frac{p}{\alpha}\frac{\partial}{\partial x}\left(\frac{p}{\rho}\right) \tag{C17}$$

where

$$\tau_{CE} = \frac{3-\gamma}{\alpha} p \frac{\partial u}{\partial x}$$

Observing that

$$\frac{\partial}{\partial x}\left(\frac{p}{\rho}\right) = -\frac{1}{2\beta^2}\frac{\partial \beta}{\partial x}$$

We can write the Chapman-Enskog distribution terms of τ_{CE} and q_{CE} as

$$f_{CE} = F\left[1 - \frac{\tau_{CE}}{p} P_\tau - \frac{q_{CE}}{p\sqrt{2RT}} P_q\right] \tag{C18}$$

where the polynomials P_τ and P_q are given by

$$P_\tau(v, I) = \frac{3\gamma - 5}{2(3-\gamma)} + C^2 - \frac{4(\gamma-1)^2}{(3-\gamma)^2}\frac{I}{2RT} \tag{C19}$$

$$P_q(v, I) = \frac{2(\gamma-1)}{\gamma}\left[C^3 - \frac{5}{2}C + \frac{4(\gamma-1)}{3-\gamma} C \frac{I}{2RT}\right] \tag{C20}$$

where

$$C = \frac{v-u}{(2RT)^{1/2}}$$

The kinetic numerical method involves integrals of f_{CE} with respect to v and I. The mass and momentum transport involves

$$\iint f_{CE}\, dv\, dI \qquad \text{and} \qquad \iint v f_{CE}\, dv\, dI$$

whereas the energy transport involves

$$\iint I f_{CE}\, dv\, dI \qquad \text{and} \qquad \iint v^2 f_{CE}\, dv\, dI$$

The dependence of I can be integrated. For 1-, v-, and v^2-transports, we then have

$$\begin{aligned} \bar{f}_{CE} &= \int f_{CE}\, dI \\ &= \tilde{F}\left[1 - \frac{\tau_{CE}}{p}\left(C^2 - \frac{1}{2}\right) - \frac{q_{CE}}{p(2RT)^{1/2}}\frac{2(\gamma-1)}{\gamma}\left(C^3 - \frac{3}{2}C\right)\right] \end{aligned} \tag{C21}$$

where

$$\tilde{F} = \frac{\rho}{(2\pi RT)^{1/2}} \exp(-C^2)$$

For I-transport,

$$\bar{\bar{f}}_{CE} = \int I f_{CE}\, dI$$
$$= \tilde{F}\left\{1 - \frac{\tau_{CE}}{p}\left[C^2 - \frac{\gamma - 1}{2(3-\gamma)}\right] - \frac{2(\gamma-1)}{\gamma}\frac{q_{CE}}{p(2RT)^{1/2}}\left(C^3 - \frac{1}{2}C\right)\right\} \tag{C22}$$

The contracted distributions $\bar{f}_{CE}$, $\bar{\bar{f}}_{CE}$, and $\tilde{F}$ do not depend on I but do depend on v. The second-order accurate KNM (eq. (58)) then reduces to

$$\begin{bmatrix} p \\ \rho u \end{bmatrix}^{n+1} = \int \begin{bmatrix} 1 \\ v \end{bmatrix} \bar{f}_{CE}(x - v\,\Delta t) dv \tag{C23}$$

$$(\rho e)^{n+1} = \int \left[\bar{\bar{f}}_{CE}(x - v\,\Delta t) + \frac{v^2}{2}\bar{f}_{CE}(x - v\,\Delta t)\right] dv \tag{C24}$$

To obtain q_{CE} and τ_{CE} in equations (C23) and (C24), α is equal to $\frac{-2}{\Delta t}$.

Appendix D

Euler Equations

The two-dimensional Euler equations for a steady flow can be written in the following form:

$$u_1 \frac{\partial \rho}{\partial x_1} + \rho \frac{\partial u_1}{\partial x_1} = -u_2 \frac{\partial \rho}{\partial x_2} - \rho \frac{\partial u_2}{\partial x_2} \tag{D1}$$

$$u_1 \frac{\partial u_1}{\partial x_1} + \frac{1}{\rho} \frac{\partial p}{\partial x_1} = -u_2 \frac{\partial u_2}{\partial x_2} \tag{D2}$$

$$u_1 \frac{\partial u_2}{\partial x_1} = -\frac{1}{\rho} \frac{\partial p}{\partial x_2} - u_2 \frac{\partial u_2}{\partial x_2} \tag{D3}$$

$$u_1 \frac{\partial p}{\partial x_1} + \rho a^2 \frac{\partial u_1}{\partial x_1} = -u_2 \frac{\partial p}{\partial x_2} - \rho a^2 \frac{\partial u_2}{\partial x_2} \tag{D4}$$

where

$$a^2 = \gamma RT$$

The only difference between the above equations and the usual form is that all the space derivatives with respect to x_1 are on the left-hand side and all the space derivatives with respect to x_2 are on the right-hand side.

Solving equations (D2) and (D4) for $\frac{\partial u_1}{\partial x_1}$ and $\frac{\partial p}{\partial x_1}$, we obtain

$$\frac{\partial u_1}{\partial x_1} = -\frac{u_1 u_2}{u_1^2 - a^2} \frac{\partial u_1}{\partial x_2} + \frac{a^2}{u_1^2 - a^2} \frac{\partial u_2}{\partial x_2} + \frac{u_2}{\rho \left(u_1^2 - a^2\right)} \frac{\partial p}{\partial x_2} \tag{D5}$$

$$\frac{\partial p}{\partial x_1} = \frac{\rho a^2 u_2}{u_1^2 - a^2} \frac{\partial u_1}{\partial x_2} - \frac{\rho a^2 u_1}{u_1^2 - a^2} \frac{\partial u_2}{\partial x_2} - \frac{u_1 u_2}{u_1^2 - a^2} \frac{\partial p}{\partial x_2} \tag{D6}$$

Substituting for $\frac{\partial u_1}{\partial x_1}$ and $\frac{\partial p}{\partial x_1}$ in equation (D1) and simplifying, we get

$$\frac{\partial \rho}{\partial x_1} = -\frac{u_2}{u_1} \frac{\partial \rho}{\partial x_2} + \frac{\rho u_2}{u_1^2 - a^2} \frac{\partial u_1}{\partial x_2} - \frac{\rho u_1}{u_1^2 - a^2} \frac{\partial u_2}{\partial x^2} - \frac{u_2}{u_1 \left(u_1^2 - a^2\right)} \frac{\partial p}{\partial x_2} \tag{D7}$$

The results obtained can be written as the matrix equation

$$\begin{bmatrix} \frac{\partial \rho}{\partial x_1} \\ \frac{\partial u_1}{\partial x_1} \\ \frac{\partial u_2}{\partial x_1} \\ \frac{\partial p}{\partial x_1} \end{bmatrix} = \begin{bmatrix} -\frac{u_2}{u_1} & \frac{\rho u_2}{u_1^2 - a^2} & -\frac{\rho u_1}{u_1^2 - a^2} & -\frac{u_2}{u_1 (u_1^2 - a^2)} \\ 0 & -\frac{u_1 u_2}{u_1^2 - a^2} & \frac{a^2}{u_1^2 - a^2} & \frac{a^2}{\rho (u_1^2 - a^2)} \\ 0 & 0 & -\frac{u_2}{u_1} & -\frac{1}{\rho u_1} \\ 0 & \frac{\rho a^2 u_2}{u_1^2 - a^2} & -\frac{\rho a^2 u_1}{u_1^2 - a^2} & -\frac{u_1 u_2}{u_1^2 - a^2} \end{bmatrix} \begin{bmatrix} \frac{\partial \rho}{\partial x_2} \\ \frac{\partial u_1}{\partial x_2} \\ \frac{\partial u_2}{\partial x_2} \\ \frac{\partial p}{\partial x_2} \end{bmatrix} \tag{D8}$$

With equation (D8), the space derivatives with respect to x_1 can be expressed in terms of the space derivatives with respect to x_2. The Chapman-Enskog polynomials $\bar{P}_{\mathrm{CE}}$ and $\bar{\bar{P}}_{\mathrm{CE}}$ defined by equations (102) and (103) can thus be determined only in terms of v_1, v_2, ρ, u_1, u_2, p, and the space derivatives with respect to x_2. These space derivatives can be determined by a second-order accurate differencing scheme such as a central difference formula.

References

1. Pullin, D. I.: Direct Simulation Methods for Compressible Inviscid Ideal-Gas Flow. *J. Comput. Phys.*, vol. 34, no. 2, Feb. 1980, pp. 231–244.
2. Reitz, Rolf D.: One-Dimensional Compressible Gas Dynamics Calculations Using the Boltzmann Equation. *J. Comput. Phys.*, vol. 42, no. 1, July 1981, pp. 108–123.
3. Deshpande, S. M.; and Raul, Robin: *Kinetic Theory Based Fluid-in-Cell Method for Eulerian Fluid Dynamics.* Rep. 82 FM 14, Department of Aerospace Engineering, Indian Institute of Science (Bangalore, India), July 1982.
4. Aristov, V. V.; and Tcheremissine, F. G.: The Kinetic Numerical Method for Rarefied and Continuum Gas Flows. *Rarefied Gas Dynamics,* Volume 1, O. M. Belotserkovskii, M. N. Kogan, S. S. Kutateladze, and A. K. Rebrov, eds., Plenum Press, c.1985, pp. 269–276.
5. Chapman, Sydney; and Cowling, T. G.: *The Mathematical Theory of Non-Uniform Gases.* Cambridge Univ. Press, 1964.
6. Evans, Martha W.; and Harlow, Francis H.: *The Particle-in-Cell Method for Hydrodynamic Calculations.* LA-2139 (Contract W-7405-ENG. 36), Los Alamos Sci. Lab., Univ. of California, Nov. 8, 1957.
7. Rich, Marvin; and Blackman, Samuel: *A Method for Eulerian Fluid Dynamics.* LAM 2826 (Contract W-7405-ENG 36), Los Alamos Sci. Lab., Univ. of California, Mar. 29, 1963.
8. Deshpande, Suresh M.: *On the Maxwellian Distribution, Symmetric Form, and Entropy Conservation for the Euler Equations.* NASA TP-2583, 1986.
9. Harten, Amiram; Lax, Peter D.; and Van Leer, Bram: *On Upstream Differencing and Godunov-Type Schemes for Hyperbolic Conservation Laws.* ICASE Rep. No. 82-5, 1982.
10. Kullback, Solomon: *Information Theory and Statistics.* Dover Publ., 1968.
11. Narasimha, Roddam: Asymptotic Solutions for the Distribution Function in Non-Equilibrium Flows, Part 1, The Weak Shock. *J. Fluid Mech.*, vol. 34, pt. 1, Oct. 16, 1968, pp. 1–24.
12. Chakravarthy, Sukumar R.; and Osher, Stanley: High Resolution Applications of the Osher Upwind Scheme for the Euler Equations. *Sixth AIAA Computational Fluid Dynamics Conference—Collection of Technical Papers,* July 1983, pp. 363-372.

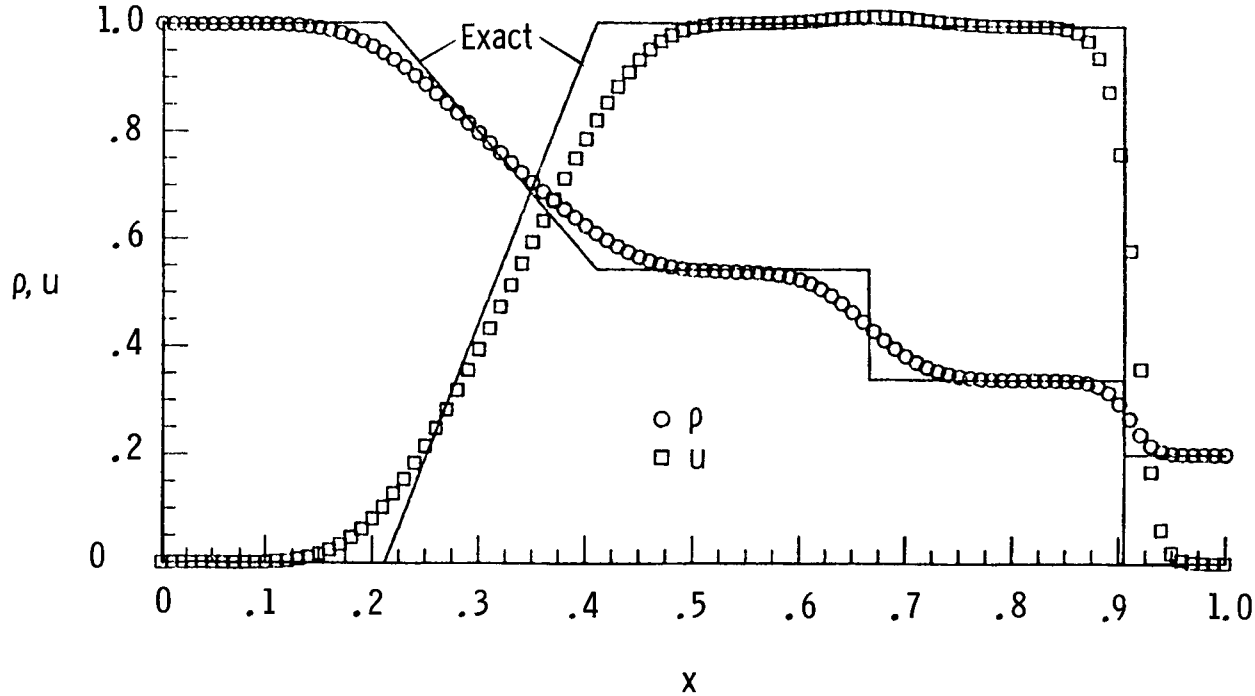

Figure 1. Computed and exact ρ and u profiles for shock-tube problem with Maxwellian ansatz. $J = 101; t_A = 0.00083$ sec.

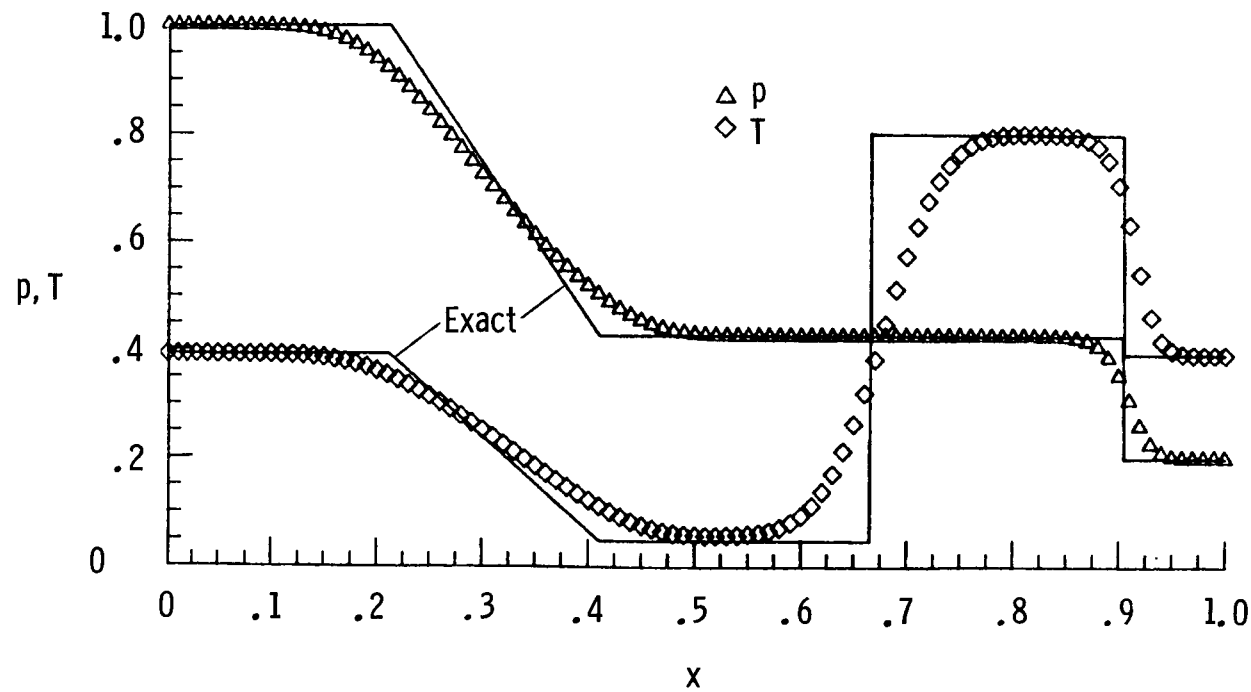

Figure 2. Computed and exact p and T profiles for shock-tube problem with Maxwellian ansatz. $J = 101; t_A = 0.00083$ sec.

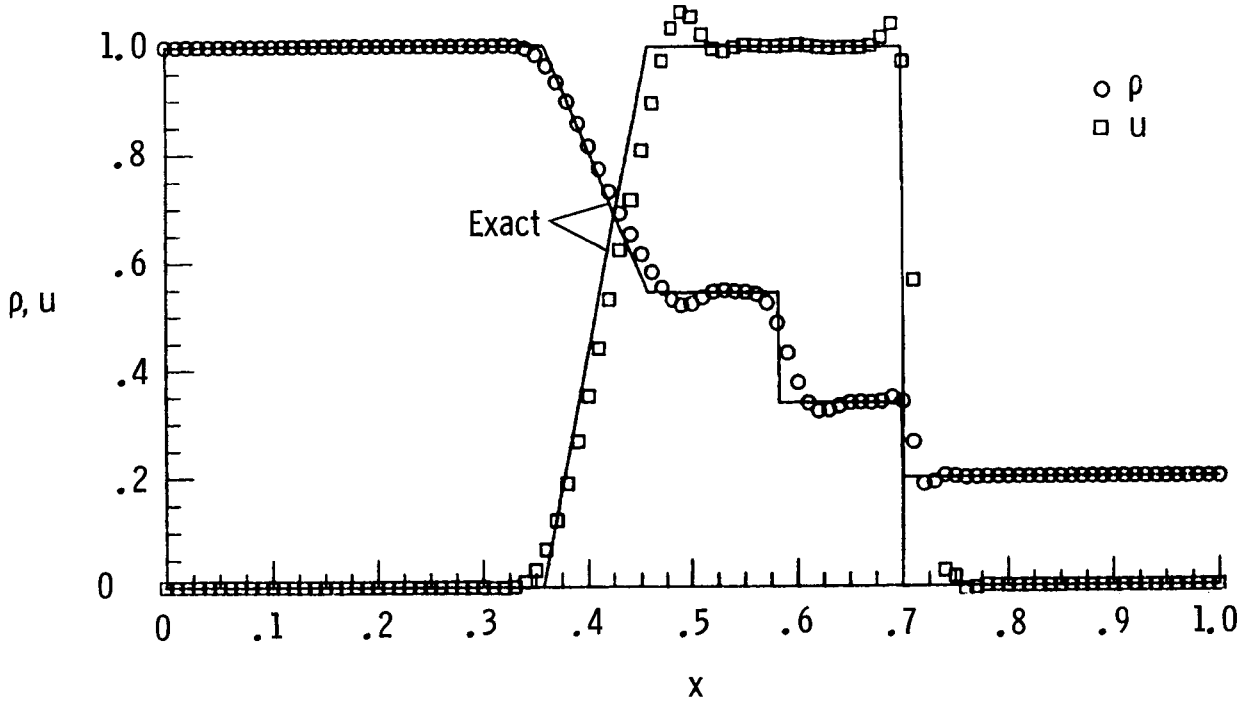

Figure 3. Computed and exact ρ and u profiles for shock-tube problem with Chapman-Enskog ansatz. $J = 101; t_A = 0.00041$ sec.

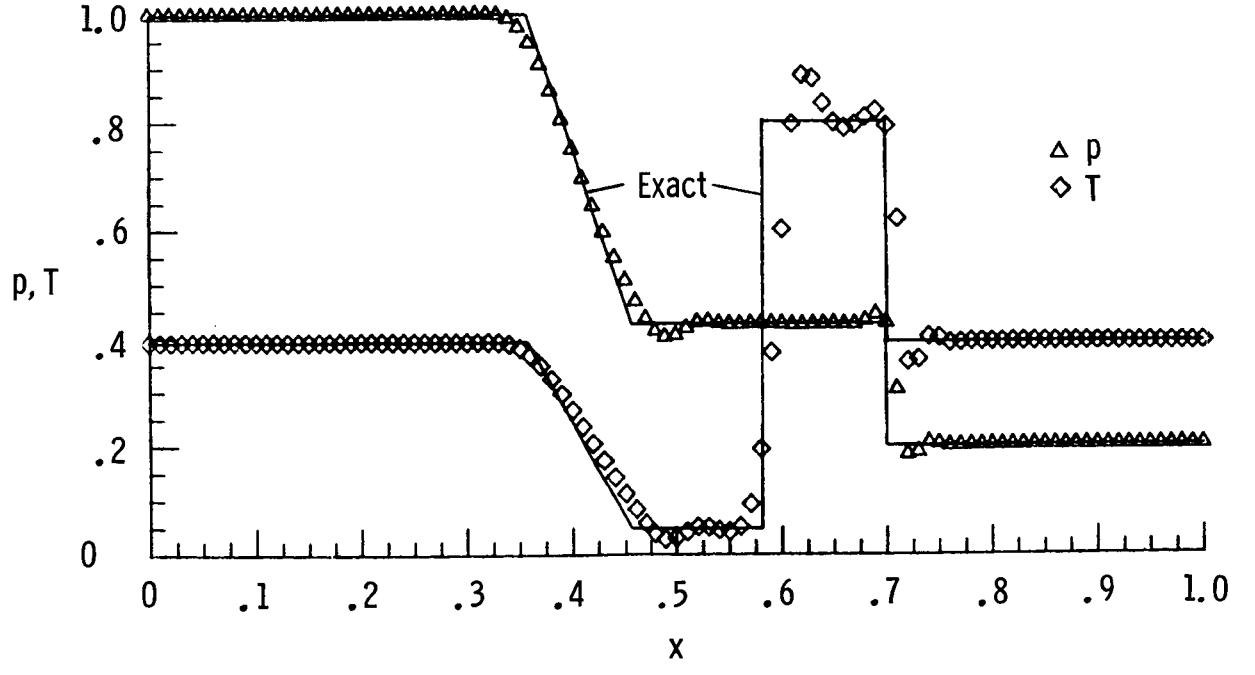

Figure 4. Computed and exact p and T profiles for shock-tube problem with Chapman-Enskog ansatz. $J = 101; t_A = 0.00041$ sec.

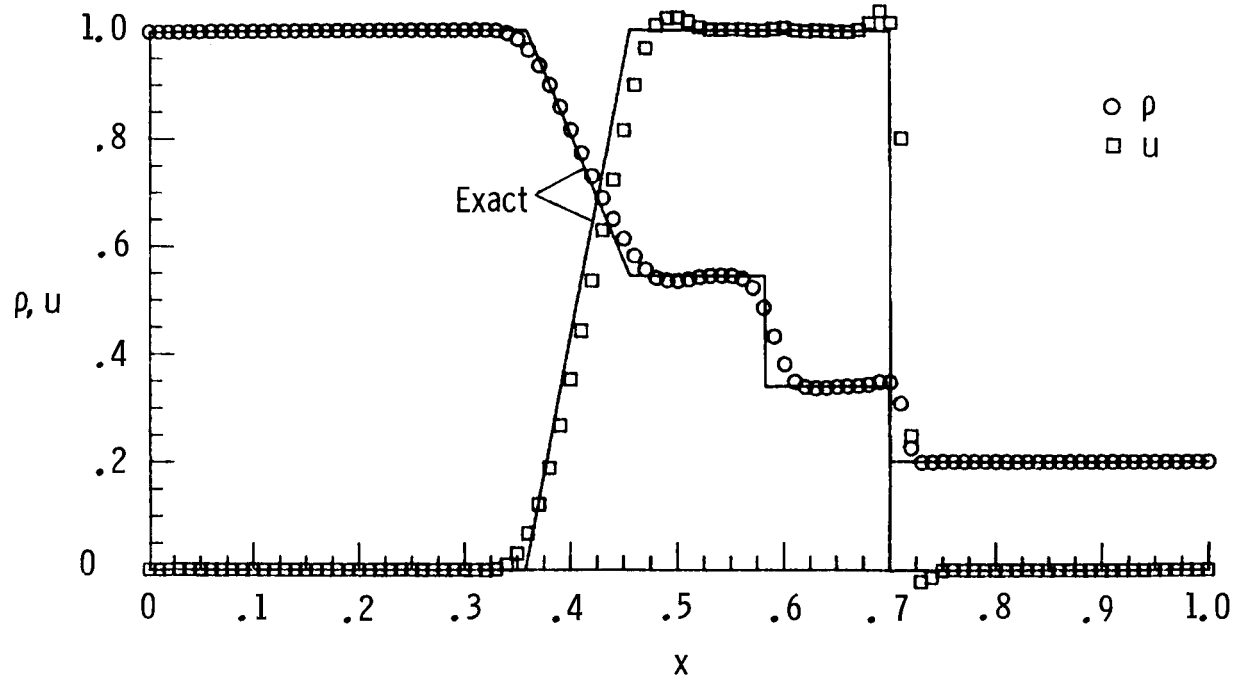

Figure 5. Computed and exact ρ and u profiles for shock-tube problem with Chapman-Enskog ansatz with TVD modification. $J = 101; t_A = 0.00041$ sec.

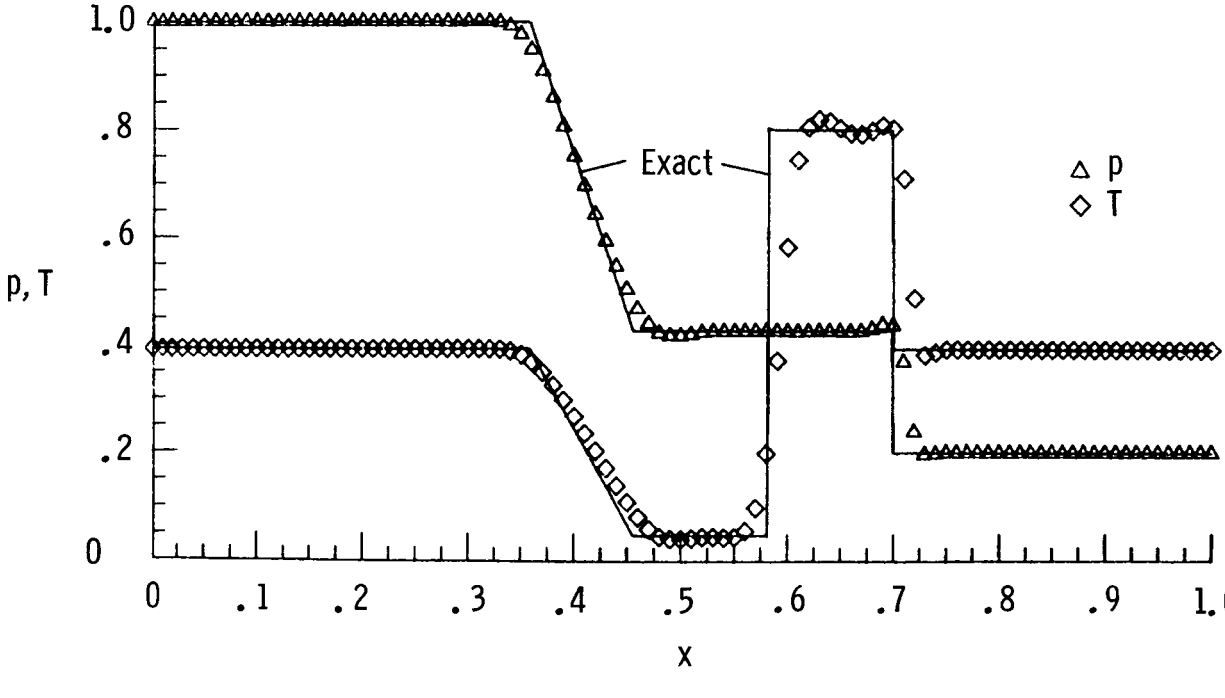

Figure 6. Computed and exact p and T profiles for shock-tube problem with Chapman-Enskog ansatz with TVD modification. $J = 101; t_A = 0.00041$ sec.

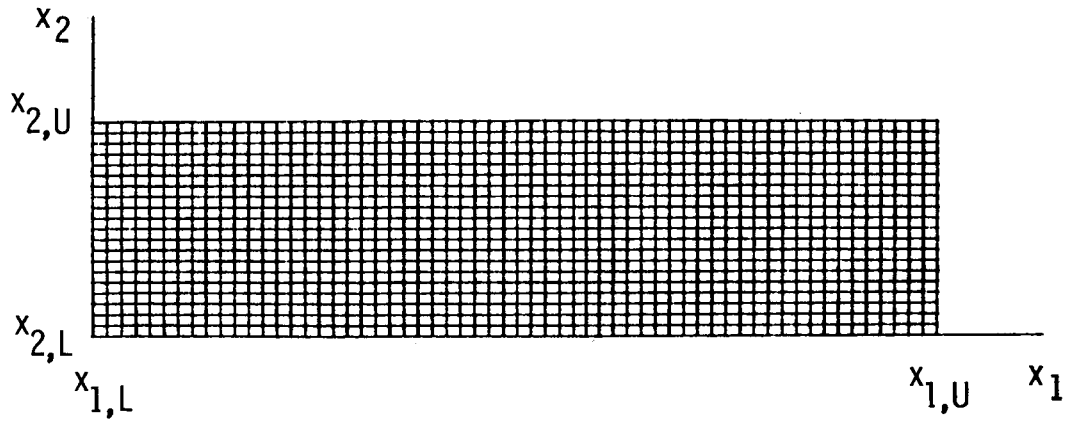

Figure 7. Computational grid with 61 × 21 points for reflection of oblique shock by a flat plate.

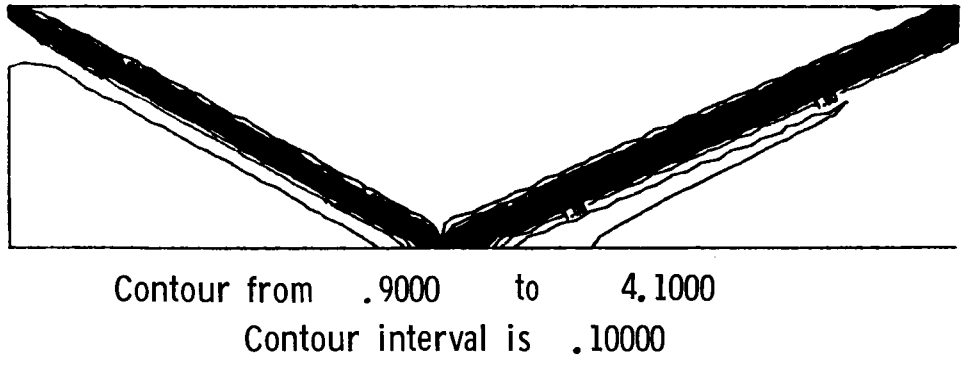

Figure 8. Pressure contours for shock-reflection problem.

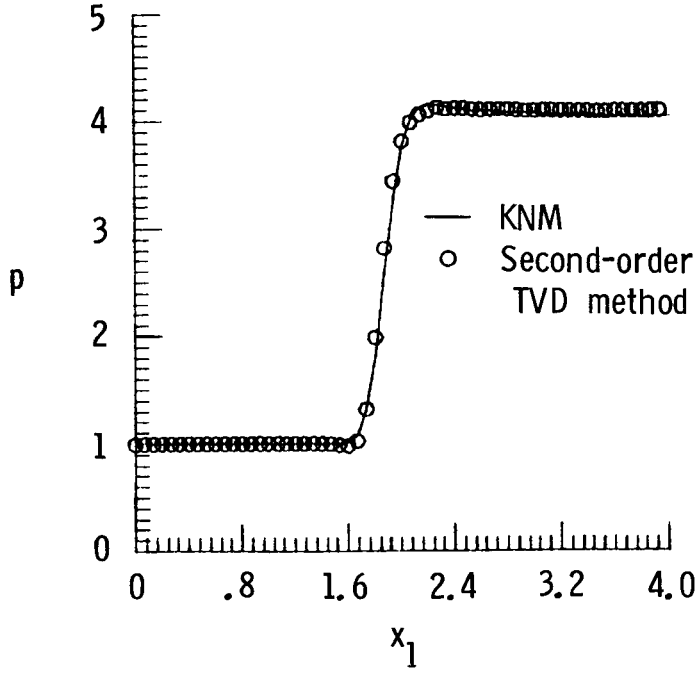

Figure 9. Pressure profiles computed with KNM and second-order TVD method for shock-reflection problem with 61×21 grid at $x_2 = 0.0$.

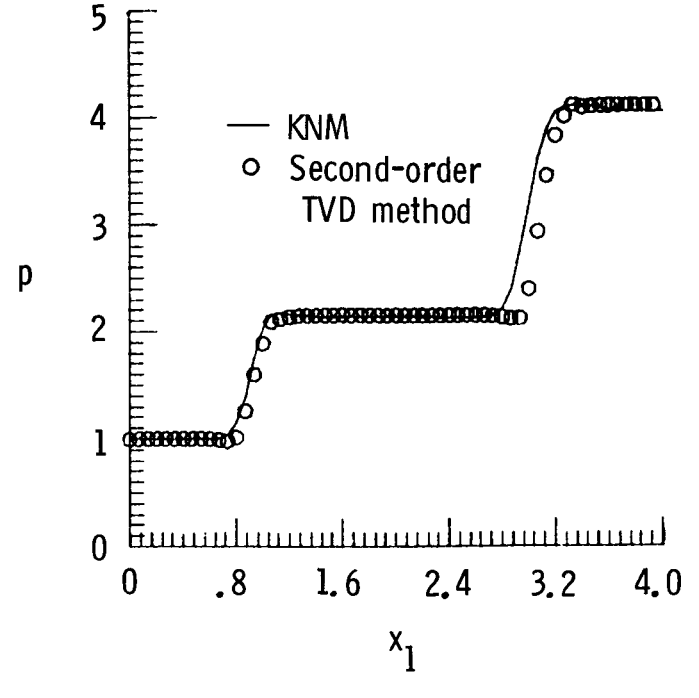

Figure 10. Pressure profiles computed with KNM and second-order TVD method for shock-reflection problem with 61×21 grid at $x_2 = 0.5$.

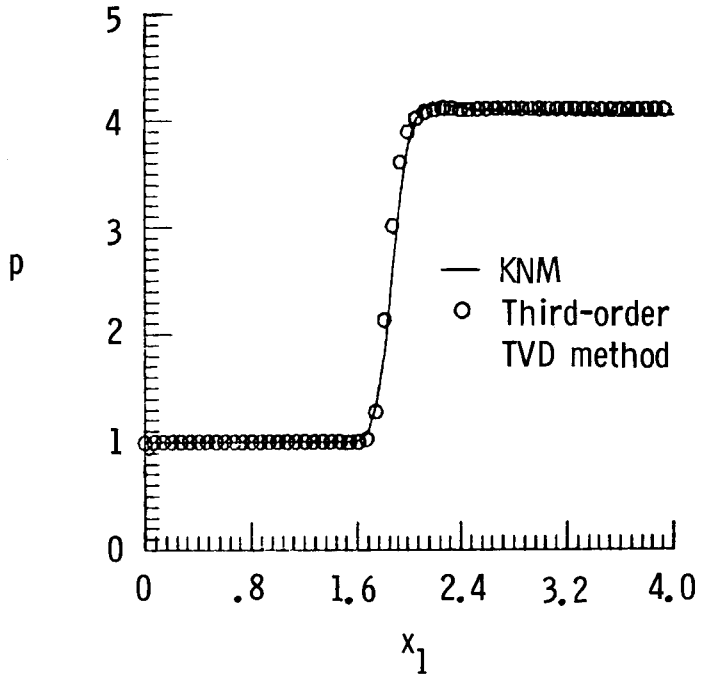

Figure 11. Pressure profiles computed with KNM and third-order TVD method for shock-reflection problem with 61×21 grid at $x_2 = 0.0$.

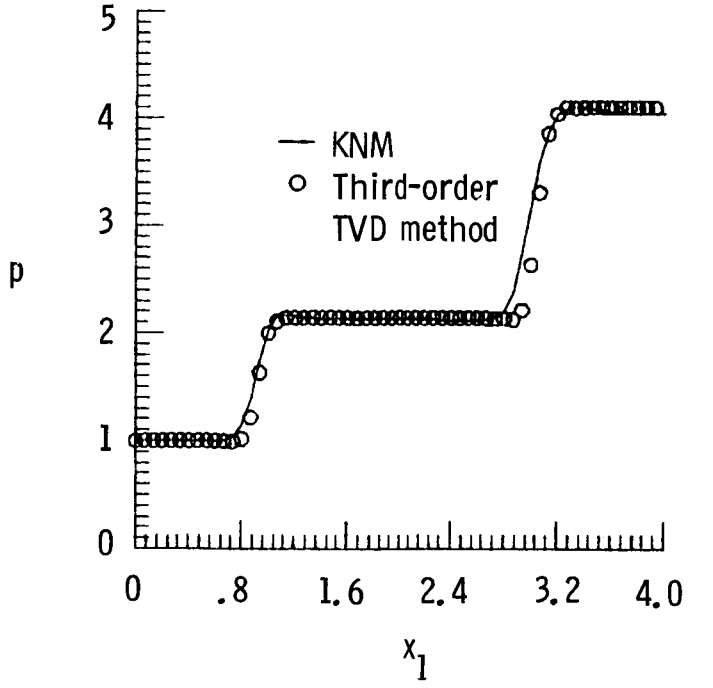

Figure 12. Pressure profiles computed with KNM and third-order TVD method for shock-reflection problem with 61×21 grid at $x_2 = 0.5$.

Standard Bibliographic Page

1. Report No.	2. Government Accession No.	3. Recipient's Catalog No.
NASA TP-2613		

4. Title and Subtitle	5. Report Date
A Second-Order Accurate Kinetic-Theory-Based Method for Inviscid Compressible Flows	December 1986
	6. Performing Organization Code: 505-31-03-02
7. Author(s): Suresh M. Deshpande	8. Performing Organization Report No.: L-16050
9. Performing Organization Name and Address: NASA Langley Research Center, Hampton, VA 23665-5225	10. Work Unit No.
	11. Contract or Grant No.
12. Sponsoring Agency Name and Address: National Aeronautics and Space Administration, Washington, DC 20546-0001	13. Type of Report and Period Covered: Technical Paper
	14. Sponsoring Agency Code

15. Supplementary Notes

Suresh M. Deshpande: NRC-NASA Resident Research Associate.

16. Abstract

A new upwind method for the numerical solution of the Euler equations is presented. This method, called the kinetic numerical method (KNM), is based on the fact that the Euler equations are moments of the Boltzmann equation of the kinetic theory of gases when the distribution function is Maxwellian. The KNM consists of two phases, the convection phase and the collision phase. The method is unconditionally stable and explicit. It is highly vectorizable and can be easily made total variation diminishing for the distribution function by a suitable choice of the interpolation strategy. The method is applied to a one-dimensional shock-propagation problem and to a two-dimensional shock-reflection problem.

17. Key Words (Suggested by Authors(s))	18. Distribution Statement
Euler equations Kinetic theory of gases Numerical method	Unclassified—Unlimited Subject Category 34

19. Security Classif.(of this report)	20. Security Classif.(of this page)	21. No. of Pages	22. Price
Unclassified	Unclassified	40	A03

For sale by the National Technical Information Service, Springfield, Virginia 22161

NASA-Langley, 1986